ABSTRACT

The Design and Synthesis of Small-Molecule Anticancer Agents Targeted Through Antibody-Drug Conjugates

James L. Kuhn

Director: Kevin G. Pinney, Ph.D.

A relatively recent addition to the arsenal of potential treatments for cancer involves the use of vascular disrupting agents (VDAs). Small-molecule VDAs target the blood supply of a tumor, starving it of nutrients and oxygen, leading to central tumor necrosis. The Pinney Group (Baylor University) has recently synthesized a variety of unique anticancer agents that function with dual modality; as potent VDAs, and as profoundly cytotoxic anti-proliferative agents. Like many cancer treatments, at a sufficiently high concentration VDAs affect healthy cells as well as malignant cells. In an effort to efficiently target these agents, such as KGP18, towards tumors and the tumor microenvironment, they are being incorporated as payloads into appropriate antibody-drug conjugates (ADCs). These constructs feature a short amino acid sequence for further selectivity along with a self-immolative spacer. The design and synthesis of these linker constructs are presented here. Future studies will determine the efficacy of these ADCs.

APPROVED BY DIRECTOR OF HONORS THESIS:

_____

Dr. Kevin G. Pinney, Department of Chemistry and Biochemistry

APPROVED BY THE HONORS PROGRAM:

_____

Dr. Andrew Wisely, Director

DATE:_____

THE DESIGN AND SYNTHESIS OF SMALL-MOLECULE ANTICANCER AGENTS TARGETED THROUGH ANTIBODY-DRUG CONJUGATES

A Thesis Submitted to the Faculty of

Baylor University

In Partial Fulfillment of the Requirements for the

Honors Program

By

James L. Kuhn

Waco, Texas

May 2014

TABLE OF CONTENTS

TABLE OF FIGURES

TABLE OF SCHEMES

ACKNOWLEDGMENTS

I would like to thank my thesis advisor Dr. Kevin G. Pinney for helping me throughout the whole process. I also would like to thank Chen-Ming Lin, the graduate student in the Pinney Group who taught me how to survive in the lab.

CHAPTER ONE

Introduction

Cancer is a disease that takes a number of forms and affects millions of people. Each year there are over a million new cases, and half a million deaths from cancer.[1] Cancer accounts for one out of every four deaths in the United States.[1] There have been countless person-hours and dollars spent on attempting to defeat it, with limited success. Recently though, there have been some major victories. Certain cancers of the blood have seen great improvements through targeted therapies such as Gleevec, which inhibits an enzyme key to the progression of chronic myelogenous leukemia.[2] Breast cancer has also seen its survival rate go steadily upward through early detection and targeted therapy such as Herceptin, which binds to a receptor overexpressed in certain patients and that is key to proliferation.[3] Different approaches such as targeting tumor vasculature,[4–6] and using antibody-drug conjugates (ADCs) have also shown promise.[7,8]

The tumor vasculature is a new and promising target for cancer treatment because tumor vasculature is not the same as normal vasculature. Tumor vasculature is different from normal vasculature in a number of ways, from its morphological properties to its chemical markers. For example, tumors promote angiogenesis, and so the vasculature surrounding them is usually in a growing state.[6] Tumors are often hypoxic, which leads to the stimulation of a number of endothelial cell growth factors to promote growth and the recruitment of angiopoietins and platelet derived growth factors (PDGFs) to enlist supporting cells.[6] Tumor vasculature is also not subject to the same amount of drug resistance as traditional tumors because the endothelial cells are not malignant or

mutated. Normal tumor cells can become resistant to a drug over time due to the high rate of mutations and replication. These differences can be taken advantage of to deprive a tumor of necessary oxygen and nutrients.

The morphology of tumor vasculature is different from any other site in the normal body. It is tortuous, poorly organized, leaky, thin-walled, and subject to dead ends and loops.[5,4] Their basement membrane is often abnormal, and the endothelial cells themselves are not shaped regularly.[4] All of these characteristics lead to an inconsistent blood flow and a higher than normal vascular permeability. Any slight differences in perfusion pressures can lead to oxygen deprivation of the tumor. Capillary blood in tumors already has a higher proportion of deoxygenated blood, so any insult to the blood flow can lead to tumor necrosis.[4] This is the main difference between normal angiogenic vasculature and tumor vasculature; one can sustain a slight decrease in blood perfusion pressure, while for the other it is catastrophic.

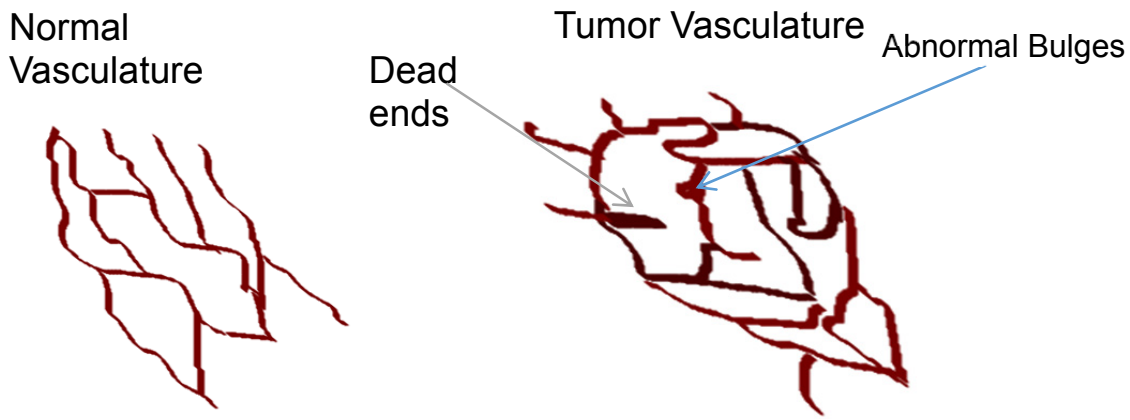

Figure 1: Normal and Tumor Vasculature

Many blood vessels in non-malignant tissues share a number of chemical biomarkers and molecules with tumor vasculature, but are not affected to the extent that tumors are by a decrease in perfusion. These markers are also only found in select regions of the body that are naturally in an angiogenic state. These markers can be used to target drugs to specific tumor regions. An example of a marker that is upregulated in angiogenic regions is the integrin family of transmembrane proteins. Angiogenic vessels have different types of integrins in comparison to resting blood vessels.[6] Integrins such as αvβ3 and αvβ5 are upregulated in cells undergoing angiogenesis, and their levels of expression on endothelial cells have been found to correlate with the grade of malignancy of neuroblastoma.[9] These markers could be used to deliver a drug conjugated to an antibody to the tumor site, or an antibody could be used to block the receptor site and affect angiogenesis. For example, blocking the α5β1 integrin results in an inhibition of angiogenesis.[6] Another example of a marker that can be exploited is the family of Vascular Endothelial Growth Factors and Receptors (VEGFs and VEGFRs).[5]

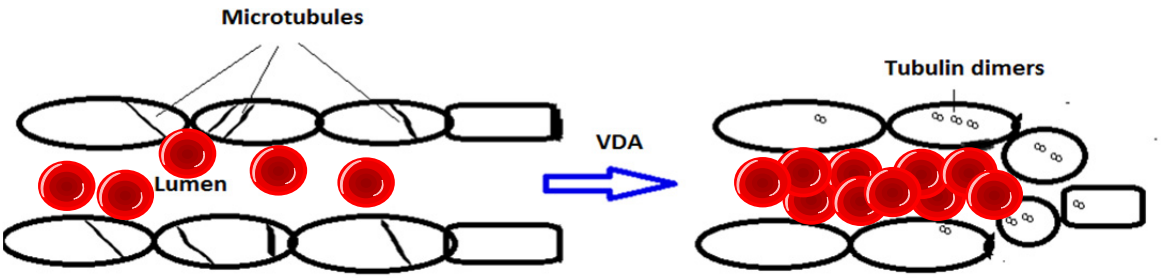

Figure 2: Effect of VDAs on epithelial cells

Brief History of the Emergence of Vascular Targeting Agents (VTAs)

In the early 1980s researchers began to realize that targeting treatments towards the vasculature of tumors might be possible and effective. It was discovered that tumor endothelial cells are almost 20 times as likely to be proliferating as regular tissue.[10] The vasculature was confirmed as a valid target when it was shown that toxins targeted to endothelial cells via an antibody caused tumor regressions in mice.[11] Tubulin binding agents were also discovered to cause vascular disruption in tumors in addition to their antimitotic effects, although for most agents the vascular effect was only observed at doses close to the maximum tolerated dose (MTD).[12] Two broad classes of VTAs emerged, ligand-directed VTAs and small-molecule VTAs. Ligand-directed VTAs work by linking a cytotoxic drug to an antibody or peptide targeted to some protein or receptor upregulated in the tumor microenvironment.[11] Small-molecule VTAs are not localized to the tumor vasculature, but instead exploit the differences in physiology and morphology between normal and tumor vasculature.[11]

Vascular Disrupting Agents (VDAs)

One class of VTAs that is showing some success against tumor vasculature is referred to as vascular disrupting agents (VDAs). These agents are very effective at reducing blood flow to tumors, although the mechanism of their specificity to tumor vasculature is not currently fully understood. Most VDAs are tubulin binding agents, which bind to tubulin and affect its regulation by inhibiting its ability to polymerize.[4]

Microtubules and the Tubulin Protein System

Microtubules are an important element of a healthy cell, they aid in cellular transport, structure, replication, and many more cellular functions. Microtubules are made up of stacked and coiled heterodimers of two related proteins called α-tubulin and β-tubulin. These tubulin dimers assemble and disassemble constantly, so that any one microtubule is constantly either losing or gaining tubulin dimers. The regulation of this process is complex and depends on many different factors to maintain 'dynamic instability'.[13] If this process is disrupted, cellular processes can grind to a halt. Cell replication cannot take place properly without microtubules to form the mitotic spindle. Many anticancer agents bind to tubulin and disrupt its activities in an attempt to disrupt cell division because cancer cells are more likely to be replicating. Tubulin binding agents that function as inhibitors of tubulin polymerization often possess dual-functionality in terms of mechanism of action. These agents typically demonstrate antiproliferative effects as well as vascular disrupting effects.

Small-molecule Vascular Disrupting Agents: Mechanism of Action

The VDAs that the Pinney Group (Baylor University) are most interested in are molecules inspired by the natural products colchicine, combretastatin A-4 (**CA4**), and combretastatin A-1 (**CA1**)(Fig. 4). These molecules bind to tubulin and inhibit microtubule polymerization. This process is thought to affect the Rho GTPase and Rho Kinase pathways (Fig. 3), because when Rho Kinase inhibitors are administered along with VDAs, the effects are much less pronounced.[5] Depolymerization of microtubules caused by VDAs leads to the activation of RhoA, which then activates RhoA Kinase

which then phosphorylates myosin.[14] Phosphorylated myosin results in increased actinomyosin contractility, an increase in cell motility, and an increase in cell detachment.[14]

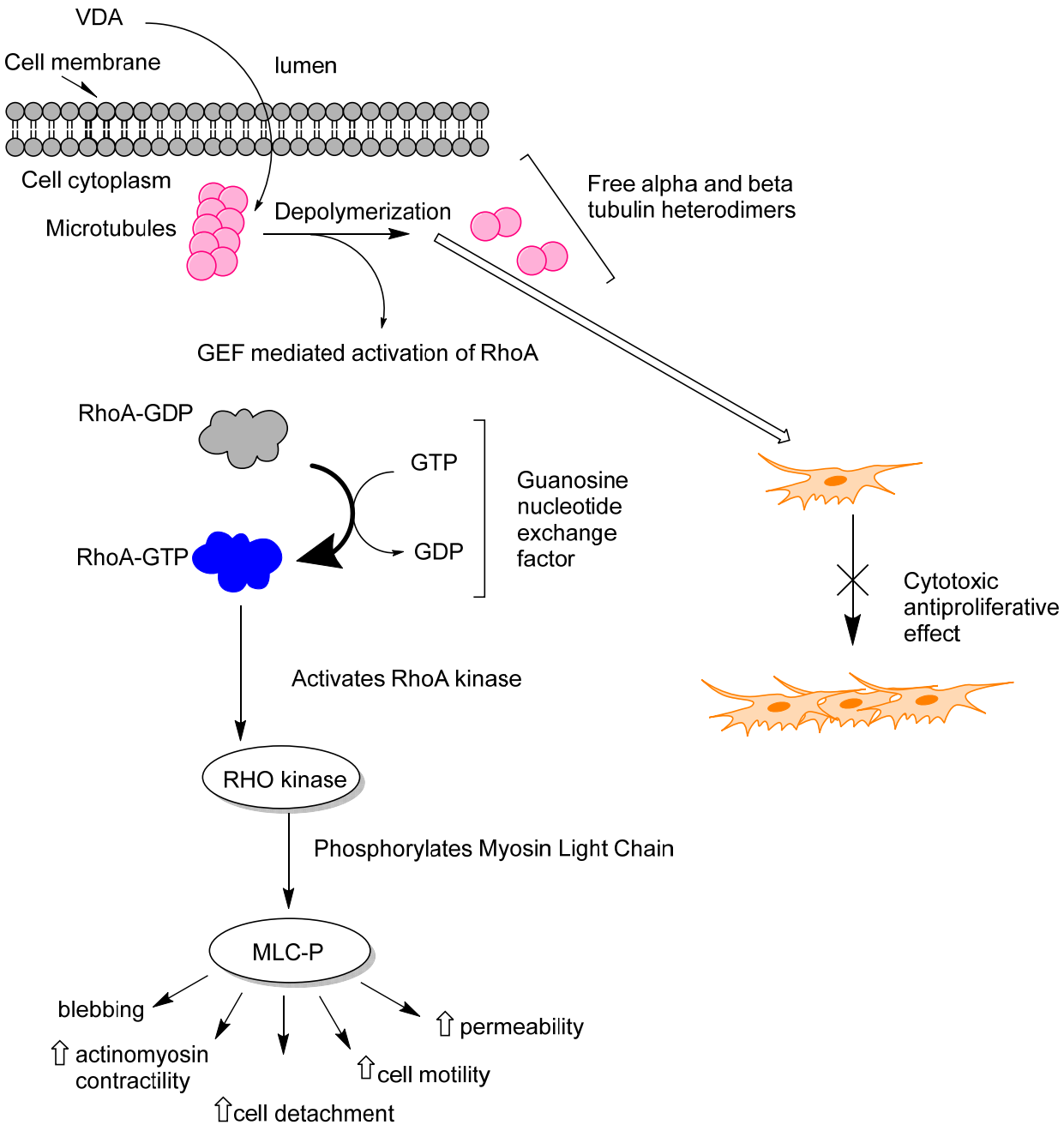

Figure 3: VDA signaling effects (Modified from Pinney and Trawick) [13]

Stress activated protein kinase p38 is also implicated as having a role in the disruption of the cell, and one combretastatin, **CA4P**, is known to activate this protein.[5] When p38 is activated it leads to blebbing of the endothelial cells and disruption of blood flow.[5]

There is also evidence that increased permeability of the tumor blood vessels is correlated with an increased sensitivity to VDAs.[5] While the exact mechanism is still unclear, it is undeniable that VDAs such as **CA4P** result in a rapid disruption of blood flow due to the blebbing of endothelial cells and their subsequent detachment from the basement membrane.[4] It also is clear that the effectiveness of tubulin polymerization inhibition is correlated with the effectiveness of the drug in disrupting vasculature. VDAs can also affect the replication of cells, halting them in the G_2/M phase, because tubulin is heavily involved in the replication process of cells. Apoptosis is only observed at concentrations much higher than those required to disrupt the blood vessels.[15] Apoptosis is not necessary though, because the disruption of the tumor blood vessels results in a drastic decrease in oxygen levels of the tumor, leading to massive and rapid necrosis.[5] The suppression of blood flow is dose dependent and lasts from 24-48 hours.[5] This effect is very noticeable and can be observed through a number of different techniques.[5]

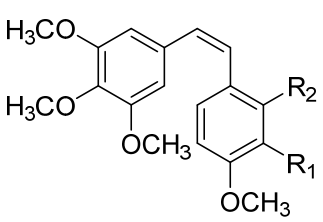

CA4: R_1= OH, R_2= H

CA4P: R_1= OPO_3^{2-} $2Na^+$, R_2= H

CA1: R_1= R_2= OH

CA1P: R_1= R_2= OPO_3^{2-} $2Na^+$

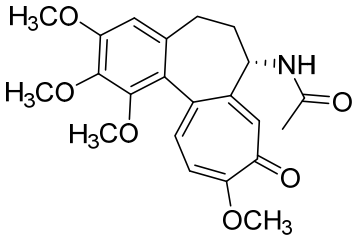

Colchicine

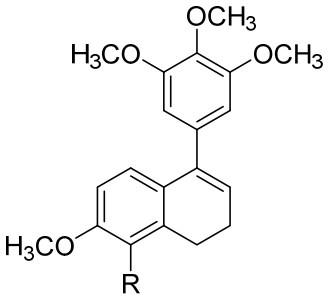

OXi6196: R= OH

OXi6197: R= OPO_3^{2-} $2Na^+$

KGP05: R= NH_2

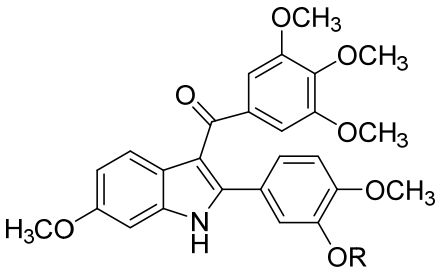

OXi8006: R= H

OXi8007: R= $PO_3^{2-}2Na^+$

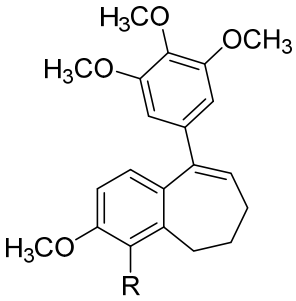

KGP18: R= OH

KGP265: R= OPO_3^{2-} Na^+

Figure 4. Representative VDAs: CA4[16], CA4P[16], CA1[16], CA1P[16], Colchicine[17], KGP18[17], OXi8006[18], OXi8007[18], OXi6196[18], OXi6197[18], KGP265[19], KGP05[20]

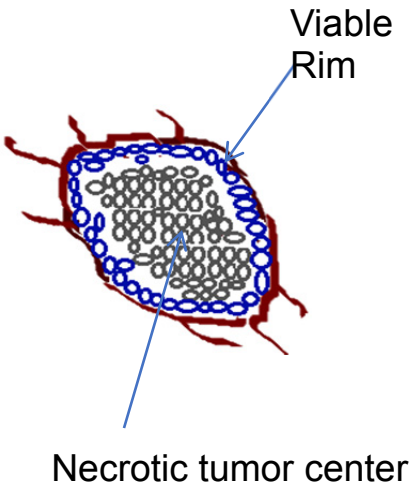

Figure 5: Viable Rim

One problem that VDAs have is that they tend to leave a 'viable rim', a number of cells surrounding the main mass of the tumor that are not affected by the vascular disruption. This is thought to be due to diffusion of nutrients and oxygen from normal surrounding vasculature,[4] as well as to differences in interstitial fluid pressure from the rim to the center. Interstitial fluid pressure is much higher in the center of a tumor, and so a slight rise in vascular permeability might be more catastrophic than on the periphery, where the interstitial fluid pressure is not so high.[4] Another potential reason for the viable rim is the tendency for a tumor to have a vascular plexus at the periphery, along with larger vessels, which are less susceptible to disruption. Unfortunately this rim is usually able to rapidly regrow the tumor, and it is hard to get a significant delay in tumor growth with only one administration of the VDA.

Because of the rim issue, VDAs have limited value as single agents. However, they show significant promise for combination therapy. Fortunately, the viable rim of a tumor is one of the few places that conventional chemotherapeutics and radiation are very effective.[4,5] The viable rim is also more accessible to antibodies, because it is well

vascularized, which could lead to the destruction of the viable rim by conventional chemotherapeutic agents conjugated to antibodies specific to the tumor. Radiation therapy is also more effective in well oxygenated areas such as the rim of a tumor because the availability of free oxygen leads to the oxidation of free radicals created by the treatment; permanently 'fixing' the DNA damage.[5] The combination of radiation therapy with a VDA has been found to lead to increased effectiveness as long as the radiation is administered prior to the VDA.[5] In fact, combination of a VDA with a conventional chemotherapeutic has also been effective, with an increase of effectiveness up to 13x over conventional drug alone.[5] The timing of VDA exposure is critical with chemotherapy as well, because if the VDA is given before the conventional drug, the drug will not be able to access as many tumor cells due to the vascular disruption.[5] The vascular disruption may also lead to drug entrapment in the tumor, leading to a longer effect on the malignant cells.[4]

Targeting Hypoxia

Another method of targeting tumor cells is through hypoxia, which is common to most solid tumors at some level. Bioreductively activatible prodrug conjugates (BAPCs) are therapeutic agents that release a free drug in low oxygen environments following bioreduction of the prodrug. An anticancer agent that is activated in hypoxic conditions would be ideal, because it would reduce negative side effects, and increase the amount that actually reaches the tumor. Hypoxia also confers resistance to some conventional therapeutic modalities, such as radiation. Hypoxic regions are three times more resistant to radiotherapy than regular cells.[21] Hypoxic cells are also less likely to be cycling, so they are more resistant to antiproliferative drugs.[21] The lack of oxygen results in a lack

of oxidation of DNA free radicals by oxygen.[22] Hypoxia also leads to genomic instability which could increase the number of mutations and potential drug resistance.[22] Hypoxia also selects for cells that are resistant to apoptosis in hypoxic conditions, which makes it more difficult to kill cells. Designing a proper tumor hypoxia targeting drug is difficult for a number of reasons. The drug must be metabolically stable enough to diffuse far from vasculature to reach severe hypoxic areas. Once it reaches a hypoxic area and is activated, it also has to be able to stay active and kill surrounding cells. This property is known as the 'bystander effect', which in the context of hypoxia activated prodrugs is defined as "the killing of adjacent cells that lack prodrug-activating ability through local diffusion of the active drug".[22] It also must be activated at the right level of O_2 saturation, too high a level and it may be activated at physiological levels. If activated at too low of a level, it will not reach areas with a low enough oxygen saturation.[22] One current drug that has shown preliminary success as a BAPC is **EO9** (Fig. 6).[23] **EO9** is an

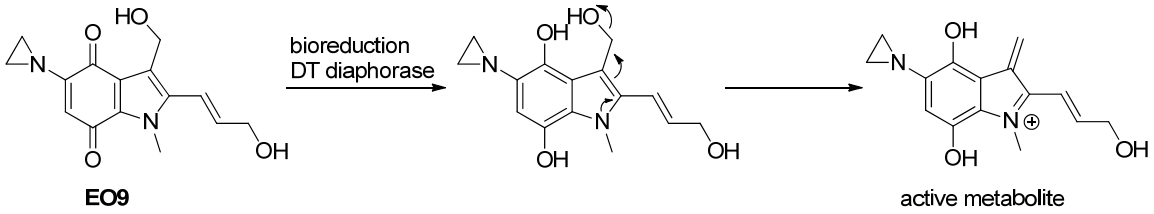

Figure 6: EO9

indolequinone that showed minimal cytotoxicity under aerobic conditions, and showed cytotoxicity at a concentration as low as 150 nM under hypoxic conditions. In comparison, the parent drug had an IC_{50} of 8.1 uM.[23] Another BAPC that uses a different mechanism for bioreduction is **TH302**, which releases a phosphoramide mustard upon bioreduction.[23]

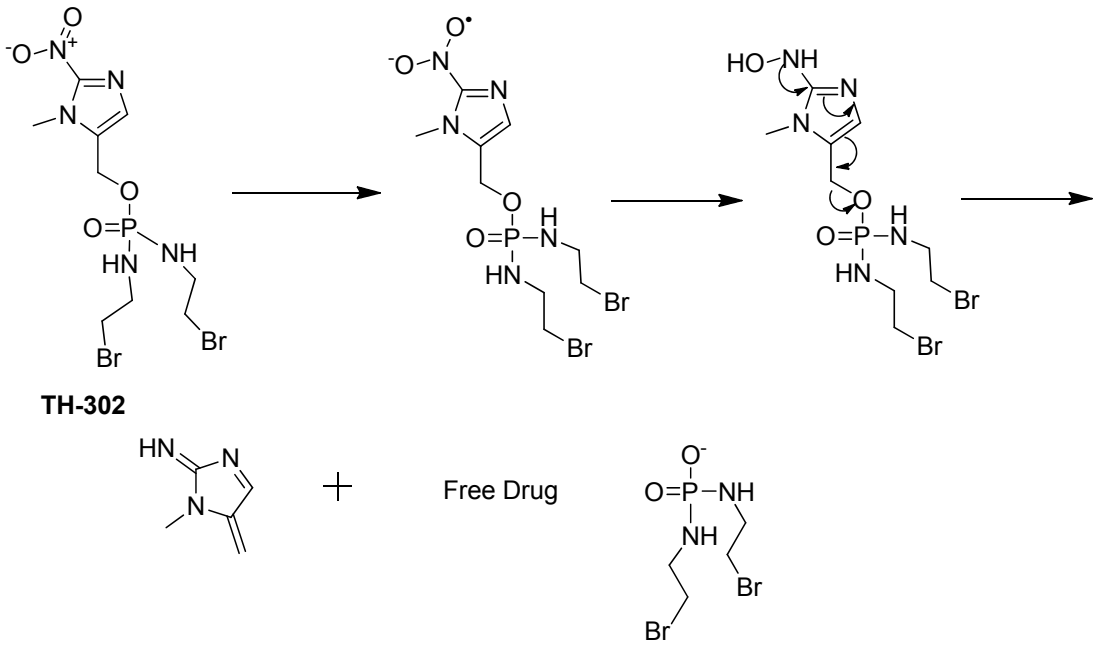

Figure 7: TH-302 bioreductive release mechanism

The BAPCs of **CA4** have shown promising results in preclinical testing as well. Some of these conjugates have shown over 40 fold selectivity to hypoxia, as measured by the hypoxia cytotoxicity ratio.[24]

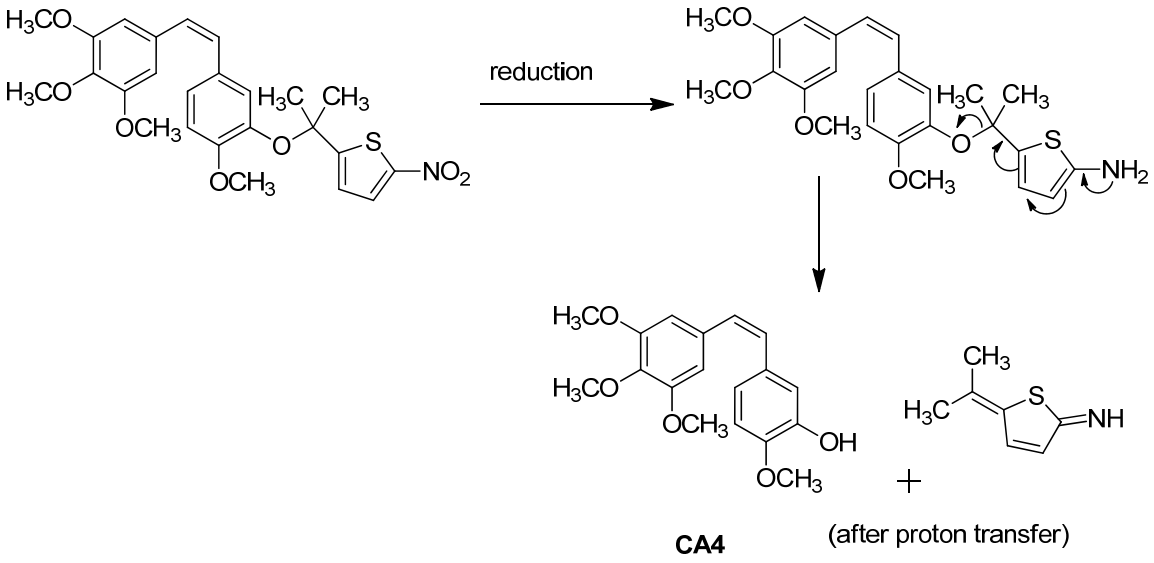

Figure 8: CA4 BAPC reduction mechanism

Cytotoxic Agents

The Pinney Group at Baylor University has recently synthesized a number of extremely potent benzosuberene analogues inspired by the natural products colchicine and **CA4**. The most potent of these is **KGP18**.[14,17,19,25,26] It was determined to have a GI_{50} of 0.0000032 uM for the DU-145 cell line.[14] In comparison, **CA4** was found to have a GI_{50} of 0.002uM for the same cell line.[14] This is extremely potent, and deserves further investigation. Previous anticancer agents in this class such as colchicine did not show vascular disrupting activity until concentrations close to their maximum tolerated dose. The synthesis of **KGP18** and its analogues went through a number of different stages

before it arrived at the synthesis used today.[14,17] The original synthetic route by the Pinney Group, while successful in yielding the desired compound, suffered from a low overall yield, due, in part, to several challenging reaction transformations including a cyanogen ring expansion reaction, a zinc reduction, and subsequent oxidation.[14,17] A research group at Pfizer discovered an alternate synthetic strategy that started from isovanillin and used a Claisen rearrangement to close the ring and a Suzuki coupling reaction to connect the trimethoxyphenyl bromide to the ketone ring.[17] Previous to this report, the Pinney Group devised a new efficient synthetic strategy that is still in use today. This new synthesis involves a Wittig reaction and uses Eaton's reagent to close the ring.[27]

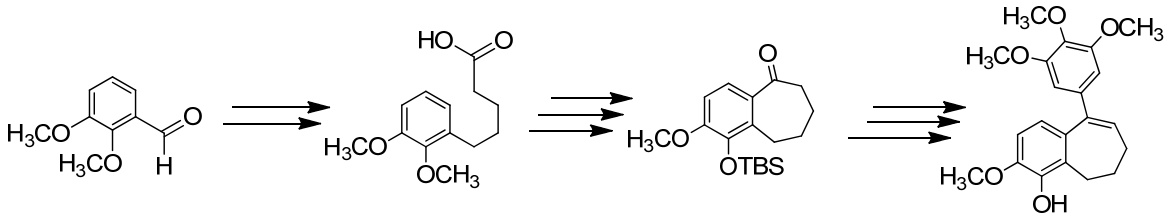

Figure 9: KGP18 synthetic route

This revised, high-yielding, robust method of Pinney and coworkers has proven consistent and has allowed for the synthesis of a number of analogues.

These benzosuberene analogues have been very effective in preclinical studies, but they are not water soluble in their active form. This has led to a number of different strategies to create water soluble prodrugs. A water soluble prodrug is desirable because it is difficult to get an insoluble substance into the bloodstream. In one approach, a phosphate salt was attached at the phenolic position (**KGP265,** Fig. 4), and this greatly increased the solubility while still allowing the free drug to be released in vivo. The body

contains a number of nonspecific phosphatase enzymes that cleave phosphate groups, and so phosphate prodrugs are typically rapidly metabolized to their active form. Another approach has been to combine the anticancer agents with antibodies, which not only increases the solubility of the drug, but allows the drug to be targeted to a specific area.

Vascular Disrupting Agents Currently in Development

Recently another drug (**BNC105P**, Fig. 10) with a structure very similar to **KGP18** was developed and went through phase 1 and 2 of clinical trials as a single agent, and is currently in a phase I/II trial with chemotherapy.[28,29] The trials of this drug,

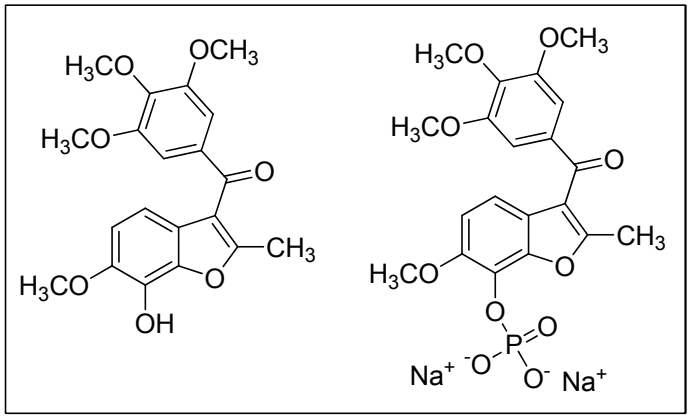

Figure 10: BNC105 and BNC105P

BNC105, can be used as a learning opportunity for future VDA development.[28,30] After reading Pinney Group patents on small-molecule agents, an Australian researcher, Bernie Flynn, synthesized Pinney Group compounds and other similar analogues with his own methodology.[31,32] Shortly thereafter he started a company, Iliad Chemicals, that was bought by Bionomics. **BNC105** was discovered by screening a number of the analogues he had synthesized for selectivity against actively proliferating endothelial cells, and **BNC105** was shown to be 80 times more potent against active endothelial cells than

against resting cells.[33] **CA4** was not shown to be selective in the Bionomics assay, although it had been previously reported to be selective.[33] The authors believed that the discrepancy was attributable to differences in cell culture conditions.[33] **BNC105** was also found to have a wider therapeutic index than CA4.[33] **BNC105** caused 95% vascular disruption at 1/8 of its No Observed Adverse Effect Level (NOAEL), while **CA4** caused only 90% vascular disruption at its NOAEL. A wide therapeutic index is key for a successful drug, especially in cancer therapy, because it means a higher dose can be given to kill the cancer without harming or killing the patient. Cancer drugs are also typically administered at or close to the maximum tolerated dose (MTD). It was discovered that **BNC105** was not a substrate for MDR-1, which is a protein frequently responsible for cancer resistance. **BNC105P** was also tested for its efficacy against tumors in mice. Twenty percent of mice had complete tumor regression, and at a level of 10 mg/kg, **BNC105P** resulted in almost complete vascular shutdown in the tumor. Because of this success, it went into clinical trials as a single agent.

In phase 1 clinical trials, **BNC105** was formulated as **BNC105P**, so that it would be more water soluble and able to be administered via an intravenous drip. During the trials, it was determined that **BNC105P** was rapidly converted into its active form in the blood stream, with a half life of 0.13 hours.[10] The trial also found that tubulin polymerization levels dropped to 1% of baseline levels, which indicates that the drug was reaching its molecular target. The trial also found that it was safe and tolerable up to a dose of 16 mg/m^2, although no objective tumor responses were observed at this level.[28] The following phase II trial also showed limited results as a single agent, as the average progression-free survival time was 1.6 months, just barely better than the progression-

free survival from best supportive care, 1.5 months.[28] The results of **BNC105P** reinforce the notion that VDAs need to be combined with other agents to reach their full potential, or need to find a way to reach higher concentrations in the tumor without causing overwhelming toxicity. Even though this drug had one of the highest selectivities towards proliferating endothelial cells in its class, and was extremely effective at suppressing tumor growth in mice, in human trials it was ineffective as a single agent. This was most likely because it did not reach a high enough concentration, or the tumor gained resistance to the drug through one of a number of different mechanisms. It is currently continuing in human trials as a combination therapy.

Another drug that is still in human trials is **CA4P** (Zybrestat), also known as fosbretabulin, which is currently in phase II/III trials. In a phase II trial in combination with bevacizumab, **CA4P** was found to improve overall survival by 52%.[34] In a phase II/III trial in combination with carboplatin and paclitaxel, it was found to triple one year survival from 9% to 27% without increasing overall toxicity significantly.[35] This is very promising for future VDA development, as combinations of other cytotoxic agents with **CA4P** have proven very effective so far as would be expected according to the mechanism of action of VDAs.

Vascular Disrupting Agent Side Effects

Even though VDAs do not cause many of the typical symptoms associated with chemotherapy, they still have the potential to cause some serious side effects that limit the dose that can be safely administered. VDAs most significant negative side effects are neurological or cardiovascular. Some of the most serious dose-limiting toxicities (DLT) observed include cardiac ischemia, QTc prolongation, dyspnea, and cerebellar ataxia.[36]

Nausea, hypertension, tumor pain, and tachycardia are known to occur.[36] One advantage over conventional chemotherapy is that the negative side effects observed with VDAs are usually acute, transient, and not cumulative.[36]

Tumor Resistance Mechanisms

Unfortunately, VDAs are not completely immune to tumor resistance. Although they do not directly affect malignant cells, the changes brought on by VDAs can improve the tumors ability to regrow from the viable rim. VDAs tendency to generate hypoxic conditions can lead to activation of NF-kb (Nuclear Factor kb) and HIF-1α (Hypoxia Inducible Factor 1a). NF-kb levels have been correlated with a worse prognosis for patient survival.[37] HIF-1α is responsible for the activation of a number of angiogenic promoters such as VEGF and a number of others. This makes it an ideal target to try to block. Some anticancer agents have recently been successful in blockading HIF-1α expression, and these could be combined with VDAs to increase their efficacy.[37]
The impact of VDAs on blood levels of circulating endothelial progenitors could also cause it to impact tumor resistance. An increase in the number of circulating endothelial progenitors (CEPs) has been observed in many tumors. CEPs are mobilized from the bone marrow and differentiate into tumor endothelial cells.[37] Blood levels of CEPs have increased upon VDA administration, which leads to them preferentially colonizing the viable rim of the tumor. This could be what is responsible for the rapid regrowth of tumors after administration of VDAs. One study found that a VEGFR-2 antibody blocked CEP mobilization and resulted in a 3 fold increase in antitumor activity.[37] Tumor associated macrophages also play a role in angiogenesis and could potentially be targeted. There is also the potential to combine angiogenesis inhibiting agents with VDAs

in order to decrease the repopulation of the tumor by the viable rim. VDAs tend to upregulate angiogenesis, and so combination with an angiogenesis inhibitor could also be effective.[37]

Antibody-Drug Conjugates (ADCs)

Another way to increase the effectiveness and lessen the toxicity of small-molecule anticancer agents is to link them to an antibody that is targeted to an antigen (a protein or receptor) that is upregulated in a tumor environment. When the anticancer agent is attached to the antibody, its activity will be significantly reduced, and so it will not have as many negative side effects. An effective antibody-drug conjugate (ADC) contains a linker that is only cleavable in the tumor or tumor microenvironment. This two-fold mechanism of selectivity-first the antibody targeting and then the tumor selective peptide cleavage- ensures the free drug will only be released at the tumor. Of course, it is difficult to find a target (antigen) that is only found in tumor cells. It is also difficult to find a linker that is stable enough to survive normal physiological mechanisms, yet sensitive enough to break down only in the environment of a tumor.

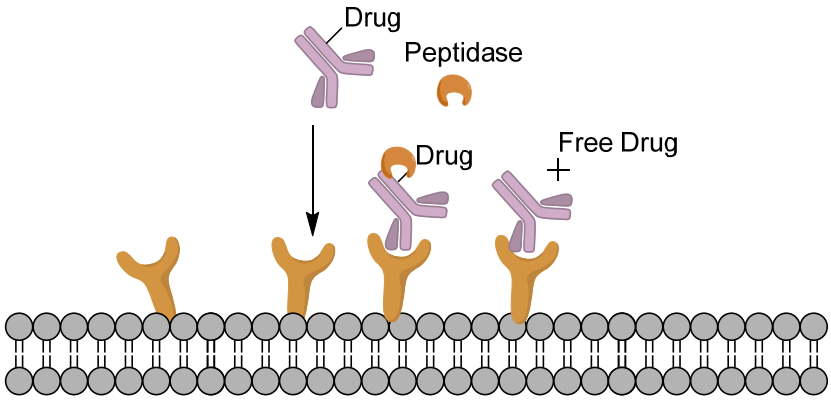

Figure 5: Antibody Drug Conjugate Release

One protein that has been found to be overexpressed in tumors is AvB_3 integrin. This protein can be targeted by a cyclic pentapeptide.[38] Another protein that has been targeted recently is plasmin, which is activated preferentially in the tumor microenvironment.[39] Because plasmin is a protease, the linker simply has to be a peptide sequence that plasmin recognizes and cleaves. The peptide sequence also has to be separated from the drug with some sort of spacer so that the protease will have room to properly cleave. Another protease that is upregulated in the tumor microenvironment is cathepsin B.[40] A significant amount of research has been done on which peptide sequences cathepsin cleaves most optimally, and it was found that it cleaves a Phe-Lys or Val-Cit sequence fastest.[40] Another compound that has been found in the tumor interstitium and lysosomes is B-glucuronidase. This enzyme cleaves B-glucuronide, and the literature has already reported some uses of B-glucuronide to link a drug and an antibody successfully.[41] There are a number of different enzymes upregulated in the tumor microenvironment that can be exploited for their cleaving specificities. It remains to be seen which of them is the most specific to tumor environments. It is possible that for different drugs different linkers may be optimal as well, due to differences in sterics and hydrophobicity.

Many linkers are conjugated to the antibody through a maleimidocaproyl group that reacts with cysteine residues in the antibody. The stability of this sulfur bridge in the biological milieu has recently been called into question. A recent study suggests that the maleimido group often exchanges with albumin in plasma, although the rate of exchange differs with the specific conjugation site residue that drug is attached to.[42] The spacer that separates the drug from the release mechanism is a key part of an effective ADC. A

spacer must be long enough to allow steric access to the release mechanism, stable enough to stay together in blood plasma and other physiological conditions, and also release quickly when triggered. There have only been a few of these mechanisms developed so far, the most widely used probably being the P-amino benzyl alcohol (PABOH). The ADC brentuximab vedotin, currently on the market, uses this mechanism to release the anticancer agent monomethyl auristatin E (MMAE). It is also known by the trade name Adcetris, contains an antibody specific to CD30, and was approved in 2011 to treat Hodgkins lymphoma and systemic anaplastic large cell lymphoma.[7]

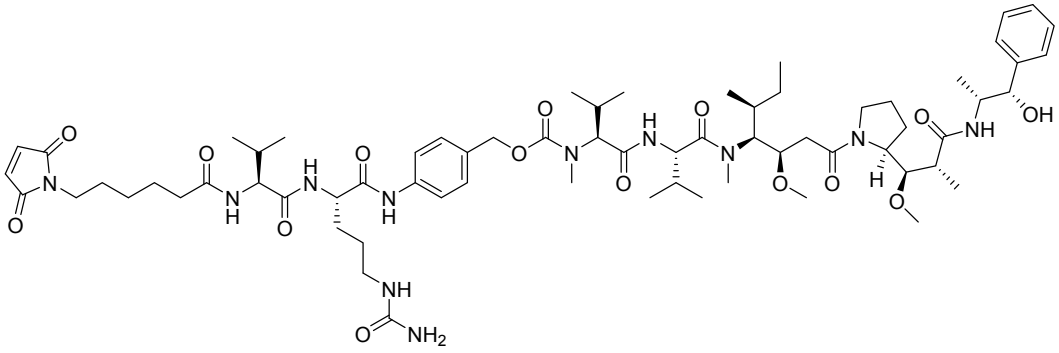

Figure 6: Adcetris

This spacer uses an electronic cascade upon cleavage to release the drug. There is a dearth of information on synthesizing a proper spacer for a phenolic drug, and this study will attempt to find a good synthetic method and spacer. It currently is unknown how stable a phenolic drug linked to PABOH would be, because it would have to be a carbonate. Carbonates are not known to be especially stable, and so it remains to be seen if the conjugate will be stable in plasma. There have been some studies on carbonate linkers that have shown them to be stable in certain cases, but none with a phenolic attachment point.[43] There also has been little data on the synthesis of phenolic

carbonates, and so this thesis will attempt to provide an effective and novel synthesis of an ADC utilizing a carbonate linker.

Amine functionalized anticancer agents are often linker through a carbamate moiety. A carbamate might be a safer bet for stability, and there is another type of linker that would allow for a phenolic drug to form a carbamate, and it is known as a dimethylethylene diamine (DMED). This spacer takes longer to release once it is triggered, and releases from the drug using a cyclization method.[43]

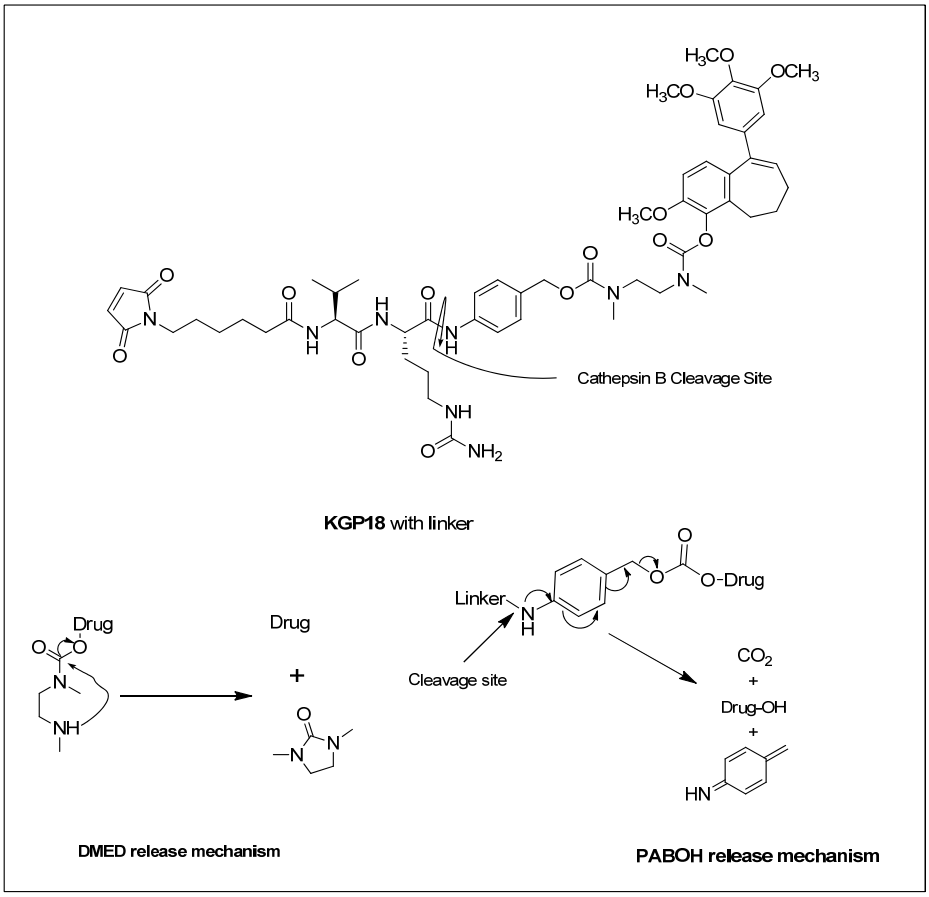

Figure 7: Self-immolative release mechanisms

Another study combined multiple linkers and found that for optimal cleavage a double PABOH was the best combination of stability and rapid cleavability.[44]

There are also some linkers that do not cleave at all. These linkers rely on the cell to internalize the ADC once it binds to a surface receptor, and then digest the antibody, leaving the drug with its linker still attached. This approach has been found to be effective in some cases, like that of ado-trastuzamab emtansine, also known as Kadcyla. The antibody target for Kadcyla is the HER2 receptor in breast cancer, and the drug payload is DM1, an extremely cytotoxic maytansine derivative.[7]

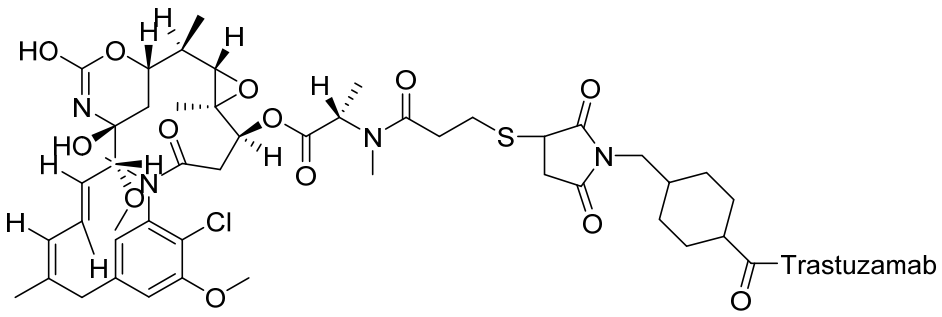

Figure 8: Kadcyla

The field of cancer research will be an exciting place over the next several years, and hopefully there will be some breakthroughs in cancer treatment. ADCs and VDAs have a lot of potential to be combined with other already existing therapies, although there needs to be work done on establishing the best administration protocols, as far as timing and what methods work best.

Statement of Purpose

A relatively recent advance in the treatment of cancer is the use of Vascular Disrupting Agents (VDAs). VDAs target the blood supply of a tumor, starving it of

nutrients and oxygen, ultimately causing central tumor necrosis. The Pinney Group (Baylor University) has recently synthesized some novel VDAs, such as **KGP18**, that are extremely potent and function with dual action. These agents have strong vascular disrupting effects and are exceptionally cytotoxic, rendering them outstanding agents for destroying cancer cells. However, like many cancer treatments, at a sufficiently high concentration VDAs potentially affect healthy as well as malignant cells.

In the interest of alleviating the potential toxicity to normal cells of these analogues and to efficiently target these agents, they are being incorporated into antibody-drug conjugates (ADCs) as payloads. These constructs feature a short dipeptide for further selectivity and a self-immolative spacer. The linker compounds were coupled with **KGP18** and other similar compounds to target the drugs to the tumor microenvironment directly, avoiding or minimizing harm to healthy cells. These linkers will eventually (in a future study) be attached to a tumor targeting antibody, creating an ADC.

VDAs and other targeted therapeutic modalities represent potentially promising anticancer treatments and thus mandate enhanced research endeavors. VDAs are powerful and effective at starving tumors of oxygen, and there is a great deal of unexplored potential for targeted anticancer agents.

This particular study has the following goals and aims:

1) Resynthesis of the potent VDA and cytotoxic agent referred to as **KGP18** in order to provide sufficient quantities for the outlined studies.

2) ADC linker strategies described in the literature will be explored in order to guide the selection and chemical synthesis of linkers suitable for the incorporation of a phenolic-based anticancer agent such as **KGP18.**
3) Synthetic efforts in conjunction with Chen-Ming Lin (graduate student in the Pinney Group (Baylor University)) will be explored to determine suitable methods for the actual covalent attachment of **KGP18** to the synthesized linker constructs.
4) Methods for characterization of the linker-conjugates and small-molecule anticancer agents synthesized in this study will include nuclear magnetic resonance spectroscopy (NMR), mass spectrometry (MS), and high pressure liquid chromatography (HPLC).
5) New chemical entities (small molecules and linker conjugates) will be evaluated biologically in future studies in collaboration with the Trawick Research Group (Baylor University).
6) Ultimately, future collaborative studies will facilitate attachment of selected antibodies to the synthesized drug-linker conjugates.

CHAPTER TWO

Materials and Methods

General Synthetic Procedures

Methylene chloride (CH_2Cl_2), acetonitrile, methanol (MeOH), ethanol (EtOH), dimethylformamide (DMF), dimethoxyethane (DME), *N*-Methyl-2-pyrrolidone (NMP), and tetrahydrofuran (THF) were used in their anhydrous form as obtained from the chemical suppliers. Reactions were performed under an inert atmosphere using nitrogen gas unless specified. Thin-layer chromatography (TLC) plates (pre-coated glass plates with silica gel 60 F_{254}, 0.25 mm thickness) were used to monitor reactions. Reactions carried out under microwave irradiation were performed with a Biotage Initiator Microwave Synthesizer. Purification of intermediates and products was carried out with a Biotage Isolera 1 or 4 flash purification system using silica gel (200–400 mesh, 60 Å) prepacked columns. Intermediates and products synthesized were characterized on the basis of their ^{1}H NMR (500 MHz) and ^{13}C NMR (125 MHz) spectroscopic data. All the chemical shifts are expressed in ppm (δ), coupling constants (J) are presented in Hz, and peak patterns are reported as singlet (s), broad singlet (bs), doublet (d), triplet (t), quartet (q), pentet (p), septet (sept), and multiplet (m). Mass spectrometry was carried out under positive ESI (electrospray ionization) using a Thermo Scientific LTQ Orbitrap Discovery instrument.

KGP05 Synthesis[20]

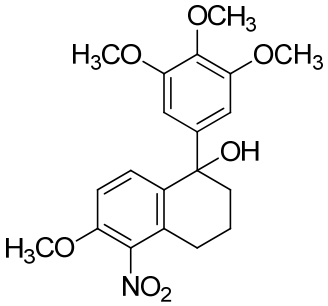

2-Methoxy-1-nitro-5-(3,4,5-trimethoxyphenyl)-6,7,8,9-tetrahydro-5H-benzo[7]annulen-5-ol (1).

To a solution of 5-bromo-1,2,3-trimethoxybenzene (1.11 g, 4.49 mmol) in THF (20 mL) at -78 °C, *n*-BuLi (1.8 mL, 2.5 M) was added and the reaction mixture was stirred for 1 h. 6-Methoxy-5-nitro-3,4-dihydronaphthalen-1(2H)-one **(**0.50 g, 2.3 mmol) in THF (3 mL) was added to the reaction mixture dropwise. The reaction mixture was stirred for 18 h and was allowed to warm to r.t. The reaction mixture was diluted with H_2O (20 mL) and extracted with dichloromethane (3 x 25 mL). The organic extract was dried over Na_2SO_4, filtered, concentrated under reduced pressure, and purified by flash chromatography (60:40 hexanes:EtOAc) resulting in alcohol **1** (0.521 g, 1.34 mmol, 59% yield)

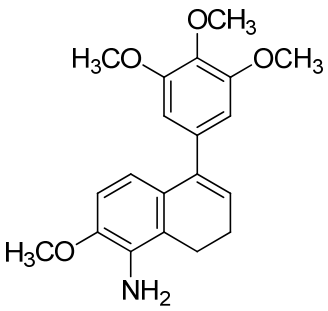

2-Methoxy-5-(3,4,5-trimethoxyphenyl)-7,8-dihydronaphthalen-1-amine (2).

Alcohol **1** (0.521 g, 1.34 mmol) was dissolved in acetic acid (18 mL) and Zn dust (1.75 g, 26.8 mmol) was added. The reaction mixture was stirred for 8.5 h, and then filtered by Celite. Filtrate was evaporated at reduced pressure, and purified by flash chromatography (70:30 hexanes:EtOAc) resulting in amine compound **2** (0.410 g, 1.27 mmol, 89% yield). **^{1}H NMR (500 MHz, $CDCl_3$)** δ 6.60 (d, *J* = 8.4 Hz, 1H), 6.56 (s, 1H), 6.51 (d, *J* = 8.4 Hz, 1H), 5.92 (t, *J* = 4.7 Hz, 1H), 5.30 (s, 1H), 3.89 (s, 1H), 3.86 (s, 1H), 3.84 (s, 3H), 2.67 (t, *J* = 7.9 Hz, 1H), 2.42 (td, *J* = 7.9, 4.7 Hz, 1H).

^{13}C NMR (125 MHz, $CDCl_3$) δ 152.93, 147.20, 140.12, 137.31, 137.04, 132.72, 128.26, 124.22, 121.21, 116.74, 107.18, 106.09, 61.06, 56.23, 55.68, 23.05, 21.74.

KGP18 synthesis[19]

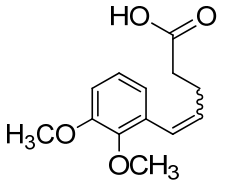

5-(2,3-Dimethoxyphenyl)pent-4-enoic acid (3).

To a solution of anhydrous THF (250 mL) under N_2 was added 3-(carboxypropyl)triphenylphosphonium bromide (10.8 g, 25.2 mmol) and potassium tert-butoxide (5.65 g, 50.4 mmol). The solution was allowed to stir for 1 h at ambient

temperature. The solution was then cooled to 0 °C and 2,3-dimethoxybenzaldehyde (4.2 g, 25 mmol) was added dropwise to the reaction mixture in anhydrous THF (5 mL), which was allowed to stir for 18 h at ambient temperature. The solution was quenched with 2 M HCl (20 mL), and the organic solvent was evaporated under reduced pressure. The aqueous phase was extracted with EtOAc (3 x 50 mL), dried over Na_2SO_4, filtered, evaporated under reduced pressure, and purified by flash chromatography (50:50 hexanes:EtOAc) to afford compound **3** (3.76 g, 15.9 mmol, 63% yield) as a mixture of E and Z isomers.

^{1}H NMR (500 MHz, $CDCl_3$) δ 7.09 – 6.93 (m, 1H), 6.87 – 6.76 (m, 1H), 6.75 (s, 1H), 6.59 (d, *J* = 11.4 Hz, 1H), 6.22 (ddd, *J* = 8.3, 7.5, 2.3 Hz, 1H), 5.74 – 5.65 (m, 1H), 3.86 (s, 1H), 3.85 (s, 1H), 3.78 (s, 1H), 3.76 (s, 1H), 2.62 – 2.51 (m, 2H), 2.51 – 2.42 (m, 1H).

^{13}C NMR (125 MHz, $CDCl_3$) δ 179.10, 179.08, 153.10, 152.91, 147.02, 146.43, 131.61, 131.50, 130.85, 129.59, 125.88, 125.50, 124.13, 123.75, 122.06, 118.13, 111.45, 111.11, 60.93, 60.72, 55.92, 55.92, 34.01 , 34.01, 28.41, 24.09.

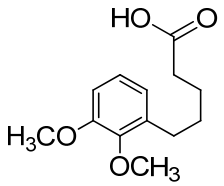

5-(2,3-Dimethoxyphenyl)pentanoic acid (4).

Compound **3** (3.76 g, 15.9 mmol) under N_2 was added to anhydrous MeOH (50 mL) under N_2. To this solution was added 10% Pd/C (0.4 g). H_2 balloons were added to the evacuated flask and the mixture was allowed to stir for 24 h. The reaction mixture was filtered through celite, washed with EtOAc (4 x 25 mL), evaporated under reduced

pressure, and purified by flash chromatography(50:50, hexanes:EtOAc) Compound **4** was obtained (3.2 g, 13 mmol, 85% yield).

^{1}H NMR (500 MHz, $CDCl_3$) δ 6.97 (t, *J* = 7.9 Hz, 1H), 6.76 (d, *J* = 8.0 Hz, 2H), 3.85 (s, 3H), 3.81 (s, 3H), 2.64 (t, *J* = 6.3 Hz, 2H), 2.37 (s, 2H), 1.77 – 1.57 (m, 4H).

^{13}C NMR (125 MHz, $CDCl_3$) δ 179.84, 152.84, 147.20, 136.01, 123.91, 121.98, 110.29, 79.39 – 75.74 (m), 60.74, 55.79, 34.09, 30.20, 29.55, 24.66.

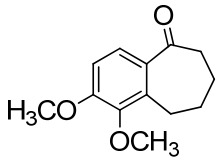

1,2-Dimethoxy-6,7,8,9-tetrahydro-5H-benzo[7]annulen-5-one (5).

To a flask containing compound **4** (10 g, 42 mmol) was added 35 mL of Eaton's reagent (10.64g P_2O_5 in 100 mL CH_3SO_3H). The solid slowly dissolved with vigorous stirring and was allowed to stir for 20 h at ambient temperature. The solution was poured over ice, which was allowed to melt, then slowly neutralized with $NaHCO_3$ (aq.). The aqueous phase was extracted with dichloromethane (2 x 25 mL). The combined organic extracts were dried over Na_2SO_4, filtered, evaporated under reduced pressure, and purified by flash chromatography (60:40 hexanes:EtOAc). Ketone **5** (6.0 g, 27 mmol, 64% yield) was obtained.

^{1}H NMR (500 MHz, $CDCl_3$) δ 7.54 (d, *J* = 8.6 Hz, 1H), 6.84 (d, *J* = 8.6 Hz, 1H), 3.91 (s, 3H), 3.80 (s, 3H), 3.03 – 2.99 (m, 2H), 2.72 – 2.68 (m, 2H), 1.88 – 1.82 (m, 2H), 1.82 – 1.75 (m, 2H).

^{13}C NMR (125 MHz,$CDCl_3$) δ 204.98, 156.20, 146.08, 135.85, 132.95, 125.59, 109.82, 61.21, 55.90, 40.76, 25.01, 23.39, 21.01.

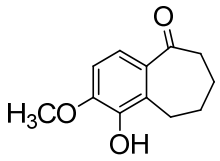

1-Hydroxy-2-methoxy-6,7,8,9-tetrahydro-5H-benzo[7]annulen-5-one(6).

Ketone **5** (1.17g, 5.33 mmol) was added to ionic liquid $[Al_2Cl_7][TMAH]$ (20.0 mL, 0.533 M). The reaction mixture was allowed to microwave at 80 °C and 1 atm for 1 h. H_2O (20 mL) was added to the mixture and the resulting brown liquid was extracted with dichloromethane (3 x 20 mL). The organic extracts were dried over Na_2SO_4, filtered, evaporated under reduced pressure, and purified by flash chromatography. (20:80 hexanes:EtOAc) Benzosuberene **6** was obtained (2.33 g, 11.3 mmol, 53% yield)

^{1}H NMR (500 MHz, $CDCl_3$) δ 7.34 (d, *J* = 8.5 Hz, 1H), 6.79 (d, *J* = 8.5 Hz, 1H), 5.77 (s, 1H), 3.94 (s, 2H), 3.11 – 2.89 (m, 2H), 2.82 – 2.62 (m, 2H), 1.84 (dd, *J* = 12.3, 5.9 Hz, 2H), 1.82 – 1.78 (m, 1H).

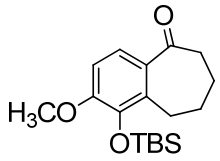

1-((*tert*-Butyldimethylsilyl)oxy)-2-methoxy-6,7,8,9-tetrahydro-5H-benzo[7]annulen-5-one (7).

To a solution of phenol **6** (1.6 g, 7.8 mmol) DMAP (0.284 g, 2.32 mmol) and Et_3N (1.64 mL, 11.6 mmol) in dichloromethane (8 mL) at 0 °C was added TBSCl (1.75 g, 11.6 mmol) in portions. The reaction mixture was stirred for 18 h, diluted with H_2O (5 mL), and extracted with Et_2O (2 × 20 mL). The organic extract was dried over Na_2SO_4, filtered, concentrated under reduced pressure, and purified by flash

chromatography (hexanes:EtOAc) to afford ketone **7** (2.20 g, 6.86 mmol, 88.5%) as a white solid

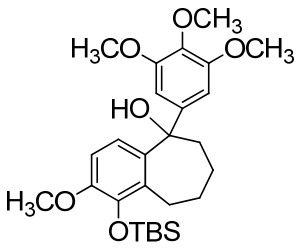

1-((t*ert*-Butyldimethylsilyl)oxy)-2-methoxy-5-(3,4,5-trimethoxyphenyl)-6,7,8,9-tetrahydro-5H-benzo[7]annulen-5-ol (8).

To a solution of 3,4,5-trimethoxyphenyl bromide (2.3 g, 9.4 mmol) in THF (50 mL) at −78 °C, *n*-BuLi (3.74 mL, 2.5 M) was added and the reaction mixture was stirred for 1 h. Ketone **7** (1.5 g, 4.7 mmol) in THF (5 mL) was added dropwise over a period of 15 min. The reaction mixture was stirred for 18 h and was allowed to warm to room temperature. The reaction mixture was diluted with H_2O (25 mL) and extracted with EtOAc (2 × 25 mL). The organic extract was dried over Na_2SO_4, filtered, concentrated under reduced pressure, and purified by flash chromatography (hexanes:EtOAc) resulting in alcohol **8** (1.59 g, 3.25 mmol, 64%)

^{1}H NMR (500 MHz, $CDCl_3$) δ 7.15 (d, *J* = 8.7 Hz, 1H), 6.70 (d, *J* = 8.7 Hz, 1H), 6.50 (s, 2H), 3.83 (s, 2H), 3.80 (s, 2H), 3.75 (s, 5H), 3.37 – 3.22 (m, 1H), 2.62 – 2.51 (m, 1H), 2.35 – 2.22 (m, 1H), 2.15 – 2.05 (m, 1H), 1.97 – 1.86 (m, 1H), 1.83 – 1.65 (m, 2H), 1.48 – 1.35 (m, 1H), 0.99 (s, 7H), 0.17 (s, 2H), 0.15 (s, 2H).

^{13}C NMR (125 MHz, $CDCl_3$) δ 153.50, 153.06, 149.36, 142.00, 138.68, 132.84, 119.78, 108.00, 104.77, 104.46, 80.08, 60.90, 56.19, 54.72, 41.40, 27.02, 26.20, 25.50, 19.03, -3.87, -4.02.

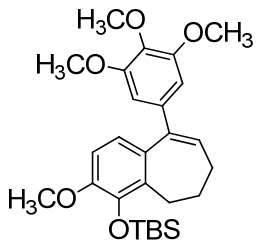

***tert*-Butyl((3-methoxy-9-(3,4,5-trimethoxyphenyl)-6,7-dihydro-5H-benzo[7]annulen-4-yl)oxy)dimethylsilane (9).**

A solution of **8** (1.5 g, 3.0 mmol) in AcOH (50 mL) was allowed to stir overnight. The reaction mixture was evaporated under reduced pressure. Reaction mixture was then diluted with water and extracted with EtOAc. The organic extract was dried over Na_2SO_4, filtered, concentrated under reduced pressure and purified by flash chromatography (hexanes:EtOAc) affording benzosuberene **9** (0.99 g, 2.1 mmol, 70%)

^{1}H NMR (500 MHz, $CDCl_3$) δ 6.69 (d, *J* = 8.5 Hz, 1H), 6.62 (d, *J* = 8.4 Hz, 1H), 6.49 (s, 2H), 6.32 (t, *J* = 7.3 Hz, 1H), 3.85 (s, 3H), 3.80 (s, 3H), 3.79 (s, 9H), 2.77 (t, *J* = 6.9 Hz, 2H), 2.11 (p, *J* = 7.0 Hz, 2H), 1.95 (q, *J* = 7.1 Hz, 2H), 1.05 (s, 9H), 0.24 (s, 6H).

^{13}C NMR (125 MHz, $CDCl_3$) δ 152.89, 148.75, 143.15, 141.57, 138.70, 137.36, 133.88, 133.33, 126.89, 122.46, 108.46, 105.33, 60.94, 56.16, 54.70, 34.02, 26.26, 25.69, 24.32, 19.11, -3.74.

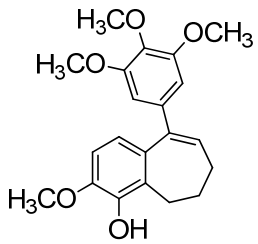

3-Methoxy-9-(3,4,5-trimethoxyphenyl)-6,7-dihydro-5H-benzo[7]annulen-4-ol (10). (KGP18)

To a solution of TBS-protected analogue **9** (1.0 g, 2.1 mmol) dissolved in THF (12 mL) was added TBAF (2.5 mL, 1 M in THF). The reaction mixture was stirred for 2 days at room temperature, concentrated under reduced pressure, and purified by flash chromatography (65:35 hexanes:EtOAc). Phenolic benzosuberene analogue **10** (0.6 g, 1.69 mmol, 80%) was obtained.

^{1}H NMR (500 MHz, $CDCl_3$) δ 6.71 (d, *J* = 8.4 Hz, 1H), 6.57 (d, *J* = 8.4 Hz, 1H), 6.50 (s, 2H), 6.34 (t, *J* = 7.4 Hz, 1H), 5.75 (s, 1H), 3.91 (s, 3H), 3.86 (s, 2H), 3.80 (s, 5H), 2.76 (t, *J* = 7.0 Hz, 2H), 2.14 (p, *J* = 7.0 Hz, 2H), 1.96 (q, *J* = 7.4 Hz, 2H).

^{13}C NMR (125 MHz, $CDCl_3$) δ 152.94, 145.19, 142.90, 142.45, 138.59, 137.43, 134.35, 127.88, 127.32, 120.94, 107.78, 105.42, 61.02, 56.25, 56.06, 33.72, 25.83, 23.66.

Linker Synthesis[45]

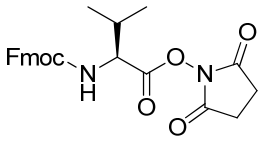

Fmoc-Val-Osu(11). Commercially available from Bachem.

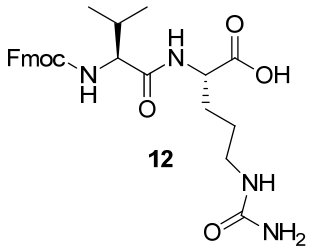

12

Fmoc-Val-Cit (12).

To a solution of Fmoc-Val-Osu (2.334 g, 5.348 mmol) in DME (14 mL) at r.t. was added a solution of L-Cit (0.9837g, 5.615 mmol) and $NaHCO_3$ (0.4717g, 5.615 mmol) in water (14 mL). THF (7 mL) was added, and the reaction was allowed to stir for 18 h. HCl was added (25 mL, 2.0 M), and the mixture was extracted with 10% isopropanol/EtOAc (2 x 50mL). The solid product began to precipitate but remained in the organic layer. The mixture was washed with water twice, the organic extract was concentrated at reduced pressure and then treated with Et_2O (50 mL). After sonication and trituration, the white solid product was collected by filtration, concentrated under reduced pressure, and dried in vacuo, yielding compound **12** (2.55 g, 5.14 mmol, 96% yield) with good yield.

^{1}H NMR (500 MHz, DMSO) δ 8.18 (d, *J* = 7.3 Hz, 1H), 7.92 – 7.55 (m, 4H), 7.53 – 7.28 (m, 4H), 5.94 (t, *J* = 5.5 Hz, 1H), 5.38 (s, 2H), 4.29 – 4.24 (m, 1H), 4.35 – 4.11 (m, 4H), 3.93 (t, *J* = 9.0, 7.2 Hz, 1H), 2.95 (q, *J* = 12.7, 6.6 Hz, 2H), 2.02 – 1.93 (m, 1H), 1.75 – 1.66 (m, 1H), 1.61 – 1.53 (m, 1H), 1.45 – 1.35 (m, 2H), 0.88 (dd, *J* = 16.4, 6.8 Hz, 5H).

^{13}C NMR (125 MHz, DMSO) δ 173.90, 171.76, 159.19, 156.52, 144.32, 141.16, 128.12, 127.54, 125.88, 120.56, 66.14, 60.28, 52.36, 47.15, 31.02, 28.83, 27.17, 19.65, 18.71.

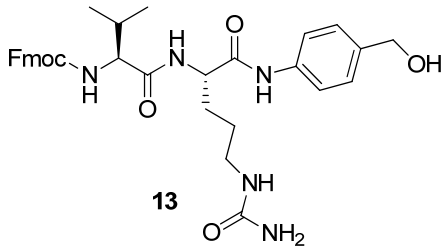

13

Fmoc-Val-Cit-PABOH (13).

P-aminobenzyl alcohol (1.19 g, 9.67 mmol) and EEDQ (2.39 g, 9.67 mmol) were added to a solution of Compound **12** (2.40 g, 4.84 mmol) in dichloromethane (48 mL) and methanol (24 mL). the reaction mixture was stirred in the dark for 1.5 days. The product **13** was afforded (2.46 g, 4.11 mmol, 85% yield)

^{1}H NMR (500 MHz, DMSO) δ 9.99 (brs, 1H), 8.11 (d, 1H), 7.92 – 7.21 (m, 12H), 5.98 (t, 1H), 5.40 (d, *J* = 17.3 Hz, 2H), 5.12 (t, 1H), 4.44 (d, 2H), 4.34 – 4.10 (m, 2H), 3.94 (t, 1H), 2.99 (d, *J* = 34.1 Hz, 2H), 2.04 – 1.93 (m, 1H), 1.73 – 1.55 (m, 4H), 1.50 – 1.34 (m, 4H), 0.89 – 0.85 (m, 6H).

^{13}C NMR (125 MHz, DMSO) δ 171.72, 170.86, 159.34, 156.59, 144.38, 144.25, 141.17, 137.91, 128.12, 127.55, 127.41, 125.85, 120.58, 119.32, 66.15, 63.07, 60.56, 53.55, 47.16, 30.93, 30.02, 27.28, 19.72, 18.77.

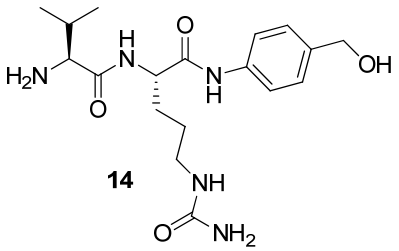

14

Val-Cit-PABOH (14).

Product **13** (8.877 g, 14.75 mmol) was dissolved in NMP (150 mL), and diethylamine was added (2 mL). The reaction mixture was allowed to stir for 16 h. The mixture was then evaporated at reduced pressure, triturated with dichloromethane, and sonicated. The

solid was collected by filtration and afforded compound **14** (5.21 g, 13.7 mmol, 93% yield)

^{1}H NMR (500 MHz, DMSO) δ 10.03 (s, 1H), 8.18 (s, 1H), 7.52 (d, *J* = 8.4 Hz, 2H), 7.22 (d, *J* = 8.4 Hz, 2H), 5.97 (s, 1H), 5.39 (s, 2H), 5.08 (s, 1H), 4.45 (s, 1H), 4.41 (s, 2H), 3.03 – 2.97 (m, 1H), 2.95 – 2.88 (m, 2H), 1.96 – 1.90 (m, 1H), 1.71 – 1.50 (m, 3H), 1.46 – 1.29 (m, 3H), 0.83 (dd, *J* = 45.9, 6.8 Hz, 6H).

^{13}C NMR (125 MHz, DMSO) δ 170.87, 159.30, 137.94, 137.85, 127.37, 119.36, 63.01, 59.95, 53.02, 31.60, 30.48, 27.14, 19.83, 17.46.

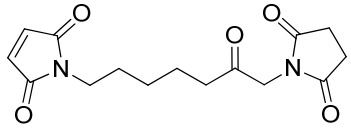

15

MC-Osu (15)

6-Maleimidocaproic acid (2.11 g, 10.0 mmol) was added to sodium carbonate (0.5 g, 5 mmol) in H_2O (100 mL). After the reactants were dissolved, the reaction mixture was evaporated. The resultant solid was then dissolved in DMF (20 mL) and disuccinimide carbonate (2.8 g, 11 mmol) was added. The reaction was allowed to stir at r.t. for 10 h. The DMF was removed at reduced pressure, then water (50 mL) was added and the product was extracted by dichloromethane (3 x 100 mL). The organic extract was then dried over Na_2SO_4, evaporated under reduced pressure, and purified by flash chromatography (MeOH/DCM) to give the product **15** (1.77 g, 5.74 mmol, 57%)

^{1}H NMR (500 MHz, $CDCl_3$) δ 6.67 (s, 1H), 3.50 (t, *J* = 7.1 Hz, 2H), 2.81 (s, 2H), 2.58 (t, *J* = 7.4 Hz, 1H), 1.75 (p, *J* = 7.5 Hz, 2H), 1.61 (p, *J* = 7.4 Hz, 2H), 1.38 (p, *J* = 7.6 Hz, 2H).

^{13}C NMR (125 MHz, $CDCl_3$) δ 170.91 , 169.25 , 168.46 , 134.15 , 37.53 , 30.84 , 28.10 , 25.90 , 25.67 , 24.14 .

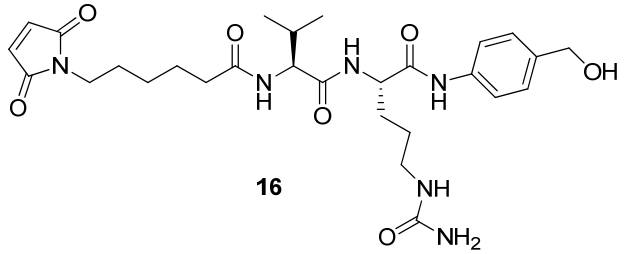

16

MC-Val-Cit-PABOH (16).

Compound **14** (1.44 g, 3.79 mmol) was dissolved in NMP (40 mL) and MC-OSu (1.3 g, 4.2 mmol) was added. The reaction was allowed to stir for 18 h. The reaction mixture was evaporated at reduced pressure and then the residue was triturated with Et_2O. The solid product was collected by filtration and washed with Et_2O. (2.42 g, 3.60 mmol, 95% yield)

^{1}H NMR (500 MHz, DMSO) δ 9.82 (s, 1H), 7.98 (d, *J* = 7.1 Hz, 1H), 7.73 (d, *J* = 8.5 Hz, 1H), 7.46 (d, *J* = 7.8 Hz, 2H), 7.14 (d, *J* = 8.0 Hz, 2H), 6.92 (s, 3H), 5.89 (s, 2H), 5.33 (s, 3H), 5.01 (s, 2H), 4.34 (s, 3H), 4.31 – 4.25 (m, 1H), 4.14 – 4.07 (m, 1H), 3.42 (s, 1H), 2.99 – 2.88 (m, 2H), 2.11 – 2.01 (m, 2H), 1.92 – 1.83 (m, 2H), 1.66 – 1.20 (m, 10H), 0.75 (dd, *J* = 15.7, 6.2 Hz, 6H).

^{13}C NMR (125 MHz, DMSO) δ 173.21, 172.69, 171.68, 171.50, 170.81, 159.29, 137.96, 137.82, 134.88, 127.34, 119.24, 63.02, 58.01, 53.50, 37.45, 35.37, 30.82, 28.21, 26.23, 25.67, 25.36, 19.70, 18.63.

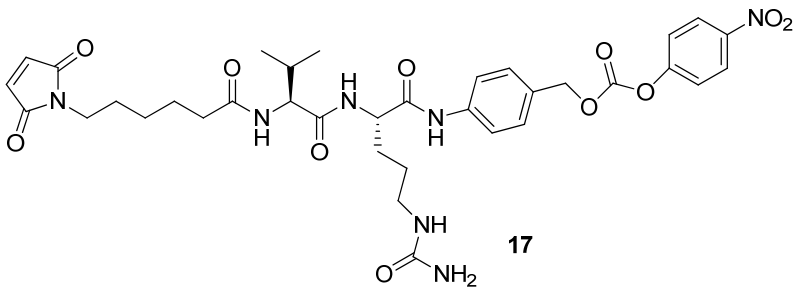

17

MC-Val-Cit-PABC-PNP (17).

Compound **16** (0.504 g, 0.880 mmol) was dissolved in DMF (5 mL) and *Bis*-PNP (1.34 g, 4.40 mmol) was added to the reaction flask. Dichloromethane was added until all reactants were dissolved. The flask was then purged and DIPEA (0.43 mL, 2.6 mmol) was injected. The reaction mixture was allowed to stir for 3 days. The DMF was removed and water was added. The product was extracted with isopropanol/EtOAc(10:90) (3 x 10 mL). After purification by flash chromatography (MeOH/DCM), the activated compound **17** (0.25 g, 0.034 mmol, 39% yield) was obtained.

CHAPTER THREE

Results and Discussion

A previously characterized benzosuberene analogue, **KGP18**, was synthesized as shown in Scheme I.[19] The synthetic procedure for this compound was already well established.[13,17,19] A Wittig reaction was used on the commercially available starting material, to afford the E/Z isomer compound **3** with 63% yield. After a high yielding H_2 gas reduction, Eaton's reagent (P_2O_5 in CH_3SO_3H) was added to compound **4** to afford ketone **5** with 85% yield. The dimethoxy ketone **5** was then subjected to a microwave reaction with ionic liquid to yield the required hydroxyl compound **6** with 53% yield. Following the TBS protection of compound **6** the resultant ketone **7** was treated with trimethoxyphenyllithium to give the tertiary alcohol **8** with 63% yield. Tertiary alcohol **8** underwent dehydration upon treatment with acetic acid to yield compound **9** in a 70% yield. Deprotection afforded 600 mg of the final compound **10**, **KGP18**. A dipeptide maleimidocaproyl linker was also synthesized to be coupled to the active compounds as shown in Scheme II.[45] Fmoc-Val-OSu was first coupled to L-citrulline to give compound **12** with 96% yield. Compound **12** was then coupled to *p*-aminobenzyl alcohol (PABOH) in the dark with *N*-ethoxycarbonyl-2-ethoxy-1,2-dihydroquinoline (EEDQ) to afford compound **13** with 85% yield. Compound **13** was then deprotected to yield compound **14** with 93% yield after trituration with dichloromethane and filtration. Compound **14** was then reacted with maleimido compound **15** and, after trituration with ether and filtration, compound **16** was obtained with 95% yield. Previous studies have determined that drug release at the target site is more efficient when the peptide cleavage site is not directly

next to the drug, possibly due to steric hindrance.[44] Because of this, multiple self-immolative linker designs were used in an attempt to link the PABOH dipeptide and the drug, although this proved to be exceedingly difficult. At first, a synthetic strategy using triphosgene was employed, attempting to activate the **KGP18** into a chloroformate, and then coupling the linker in a base catalyzed reaction, but this proved to be ineffective in many different reaction conditions (Scheme III). TLC evidence suggested that the activated **KGP18** (chloroformate) was formed, but then did not stably react with the linker, possibly reacting with itself to create a dimer. Another possibility is that the carbonate was formed, but subsequently was rapidly degraded in reaction conditions. Further test reactions are needed to determine the stability and feasibility of a carbonate linkage. A triphosgene reaction with *para*-ethylbenzyl alcohol is proposed. Another strategy that was employed involved activating the linker compound **16** using *para*-nitrophenyl (PNP) carbonate to form compound **17**, and then reacting the compound **17** with **KGP18** in basic conditions. This also proved unfruitful. Unfortunately, purification of the failed reactions was often difficult, so NMR characterization was usually not feasible to determine what side products were forming. Mass spectrometry was used to determine that no desired product was isolated. Activating **KGP18** with a PNP carbonate was also attempted. Initially *bis*-PNP carbonate was used in the attempted activation of **KGP18**, but this was unsuccessful. Later PNP chloroformate was used and was able to give the activated **KGP18**-PNP compound as determined by mass spectrometry (Scheme IV). This compound was then immediately reacted with the linker compound **16,** but no linker product was able to be obtained. Phenolic carbonates have been shown in the literature to be notoriously difficult to form efficiently.[46] Another strategy was employed

that utilized an ethylenediamine (DMED) linker to form a carbamate. The DMED linker was reacted with compound **17** in basic conditions to form an elongated linker that contained both the DMED and PABOH moieties (Scheme IV). Unfortunately, both ends of compound **17** proved to be reactive to the added DMED, and mass spectrometry evidence suggests that the linker attached at both the maleimido group and the PABOH group**.** Nonetheless, this putative compound was reacted with PNP activated KGP18, and mass spec evidence suggests 2 possible products. Future purification through crystallization hopefully will identify the product. Future studies will focus on different reaction temperatures, and different activating compounds. An *ortho*-nitrophenyl carbonate will also be attempted.

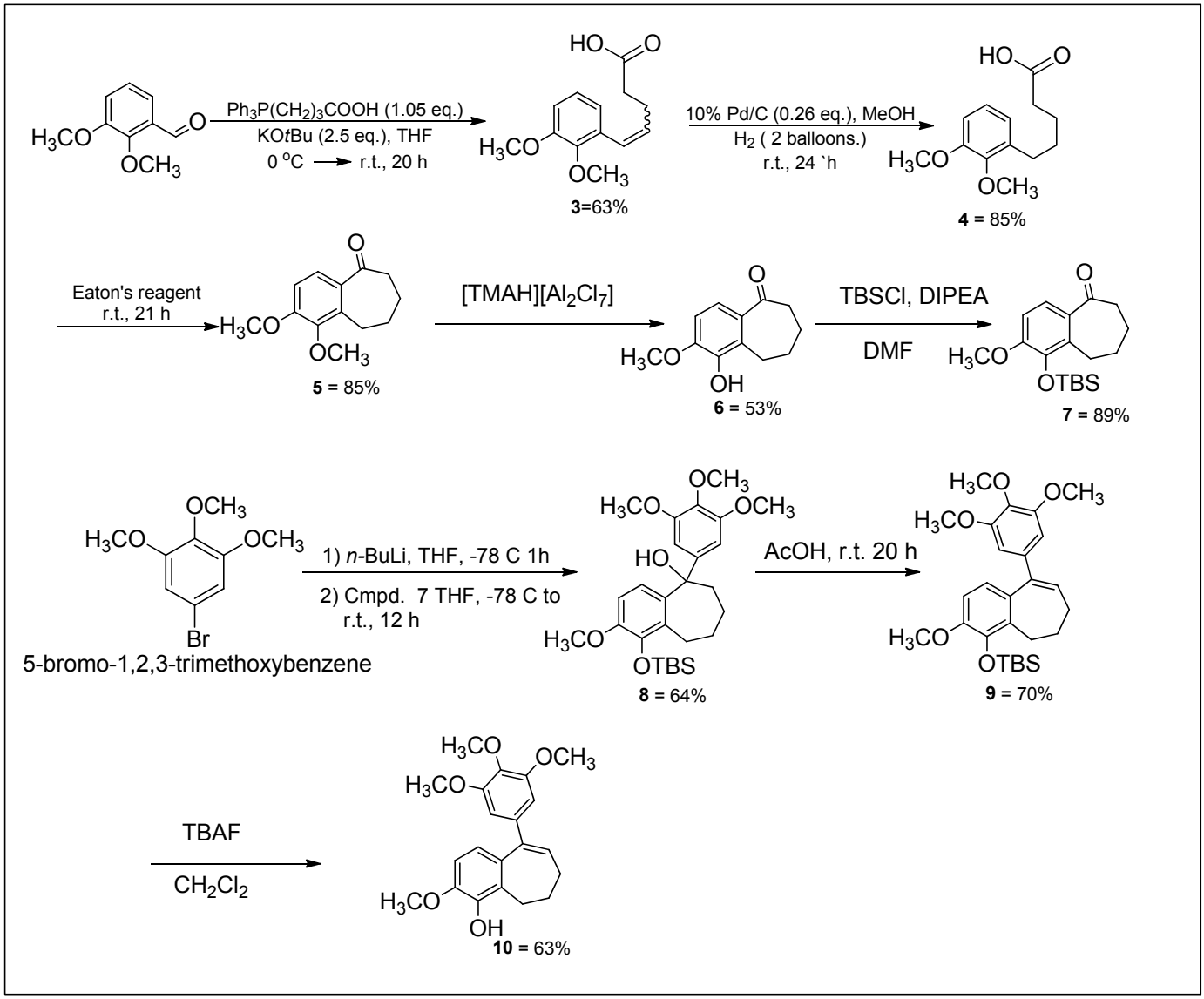

Scheme I: KGP18 synthesis

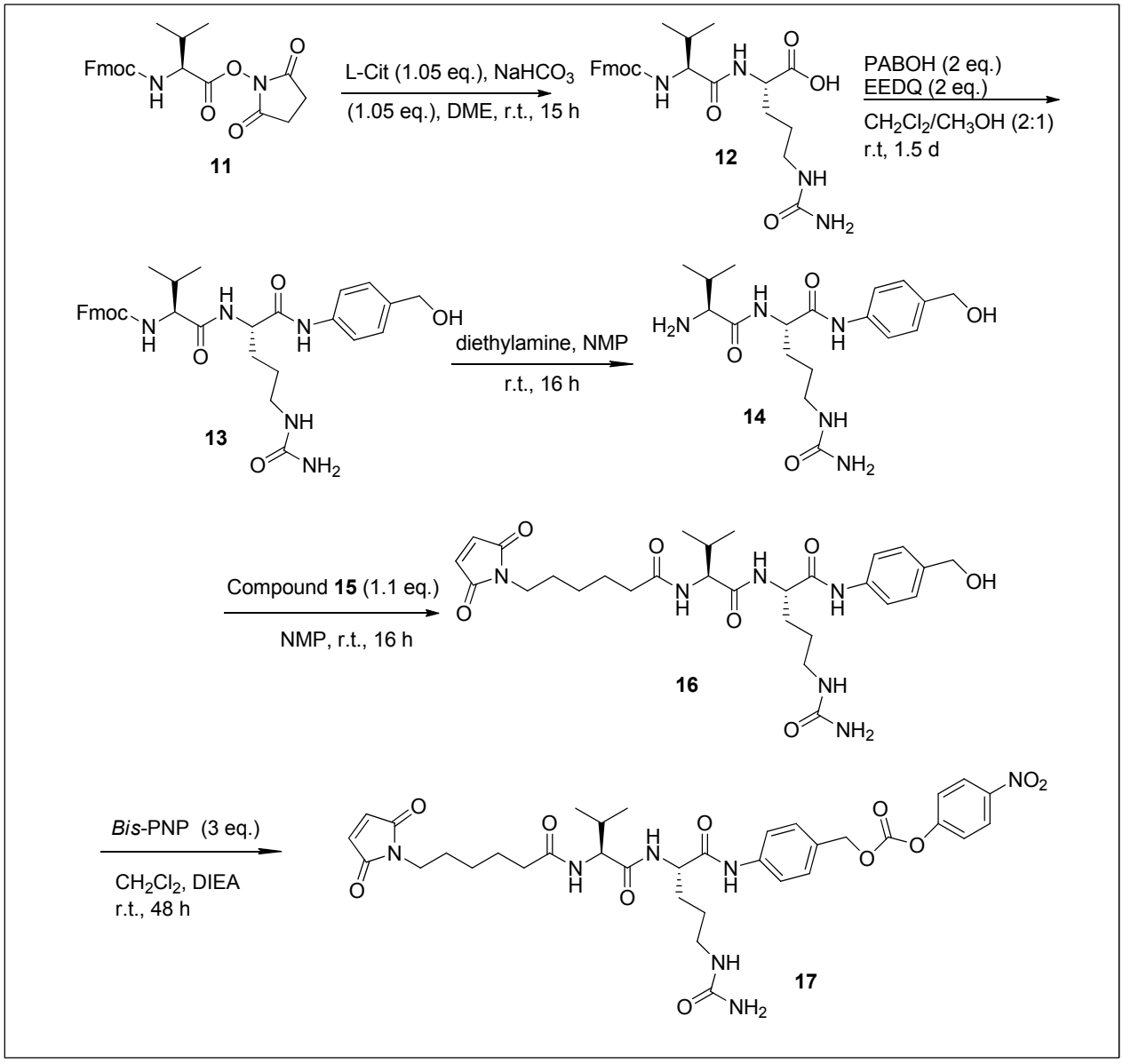

Scheme II: Linker synthesis

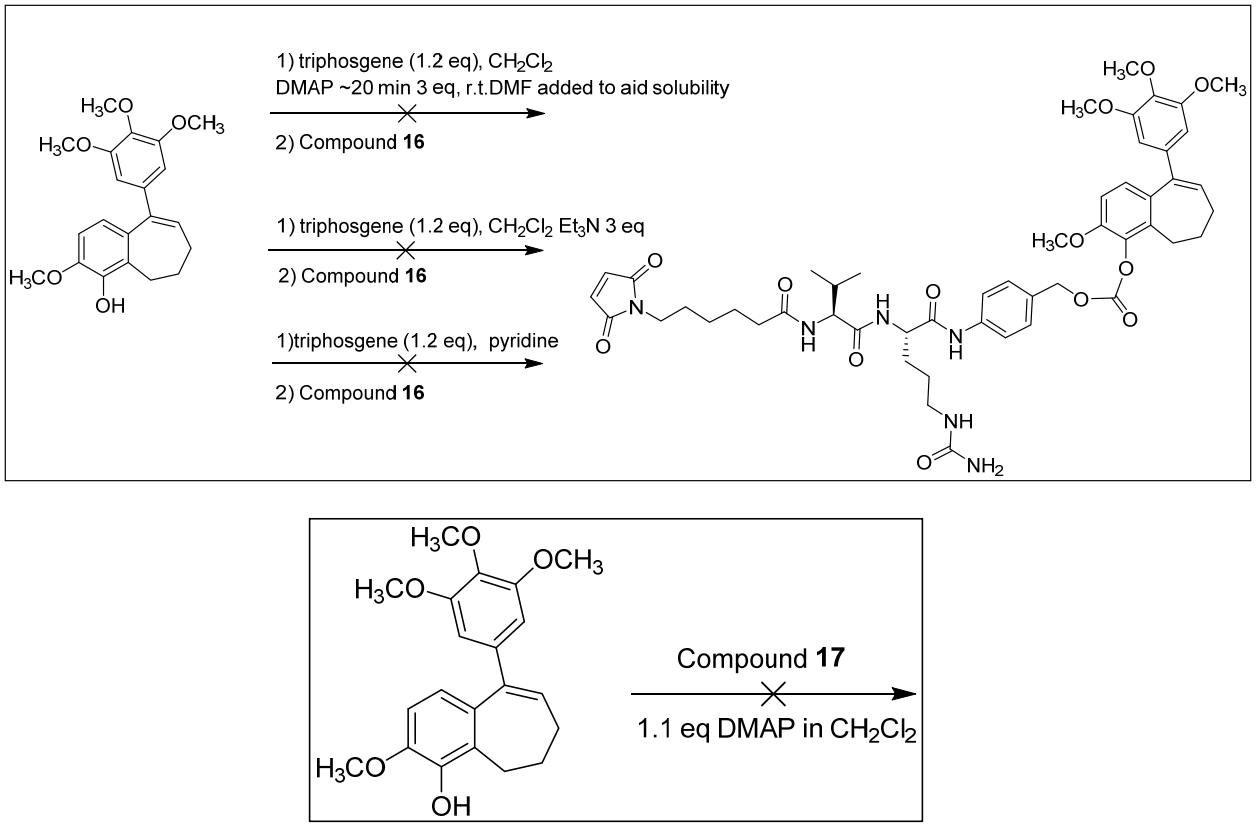

Scheme III: Attempted couplings

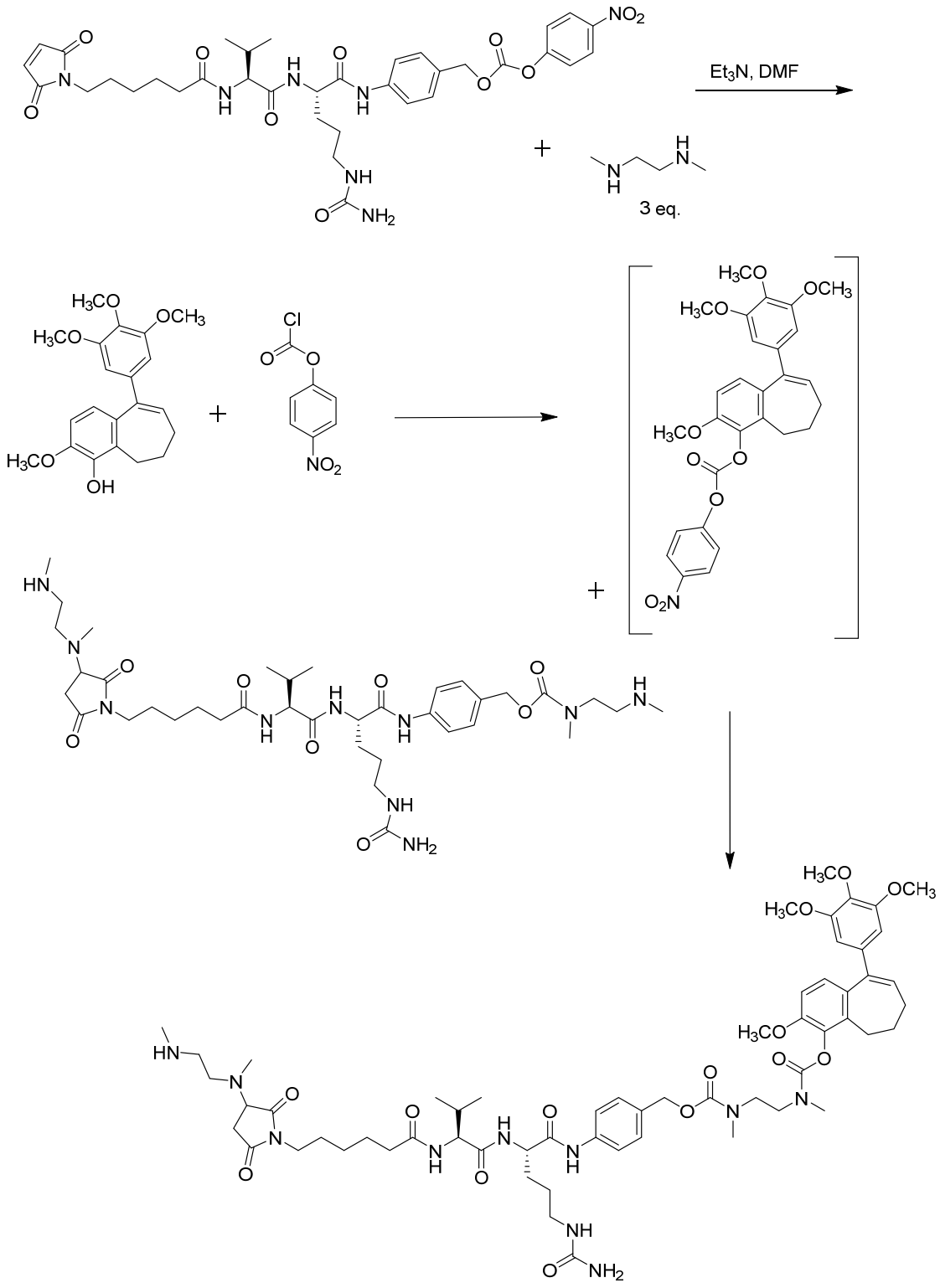

Scheme III: Revised linker coupling

APPENDIX

NMR Data

^{1}H NMR (500 MHz, $CDCl_3$) Compound 2

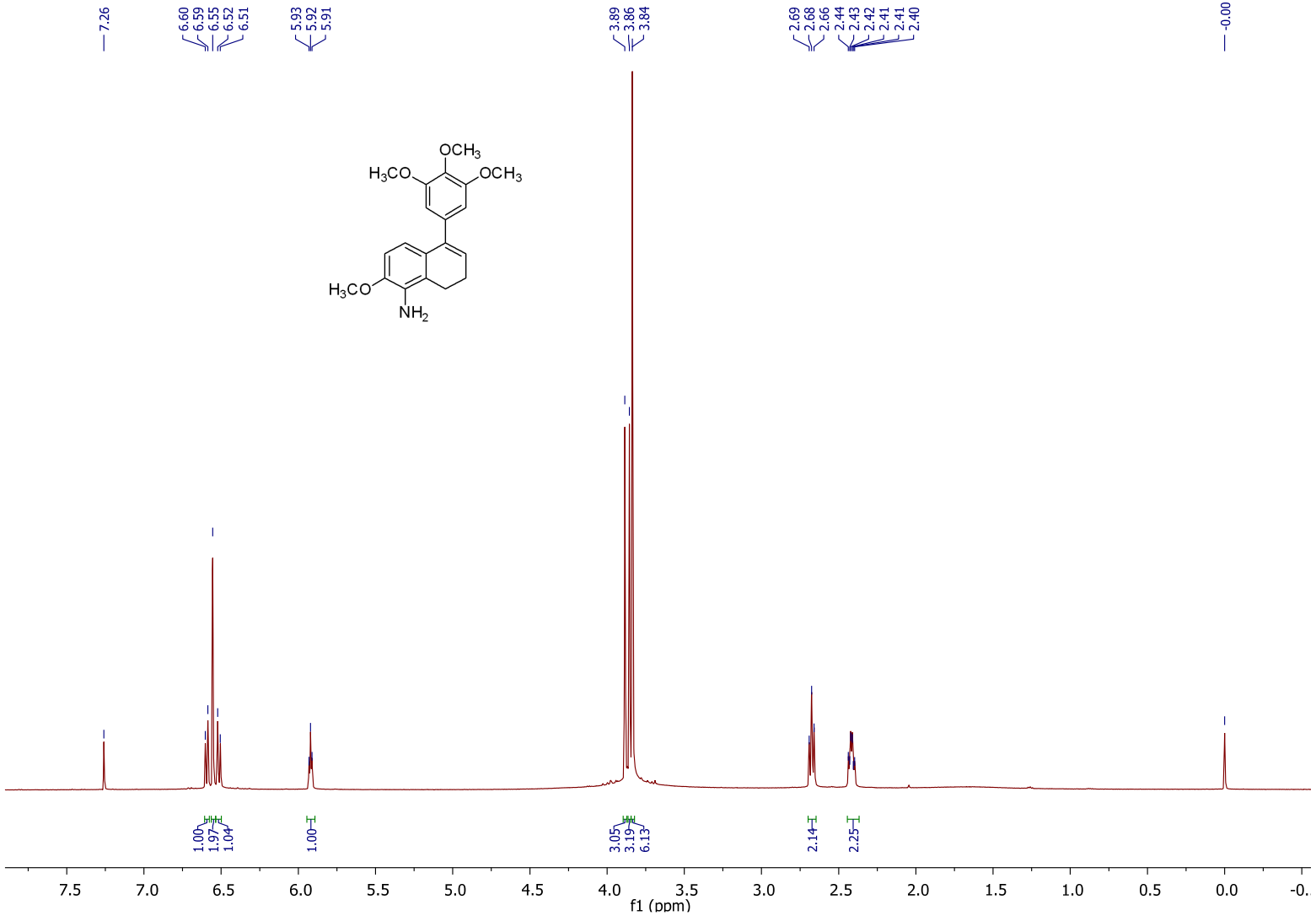

^{13}C NMR (125 MHz, $CDCl_3$) Compound 2

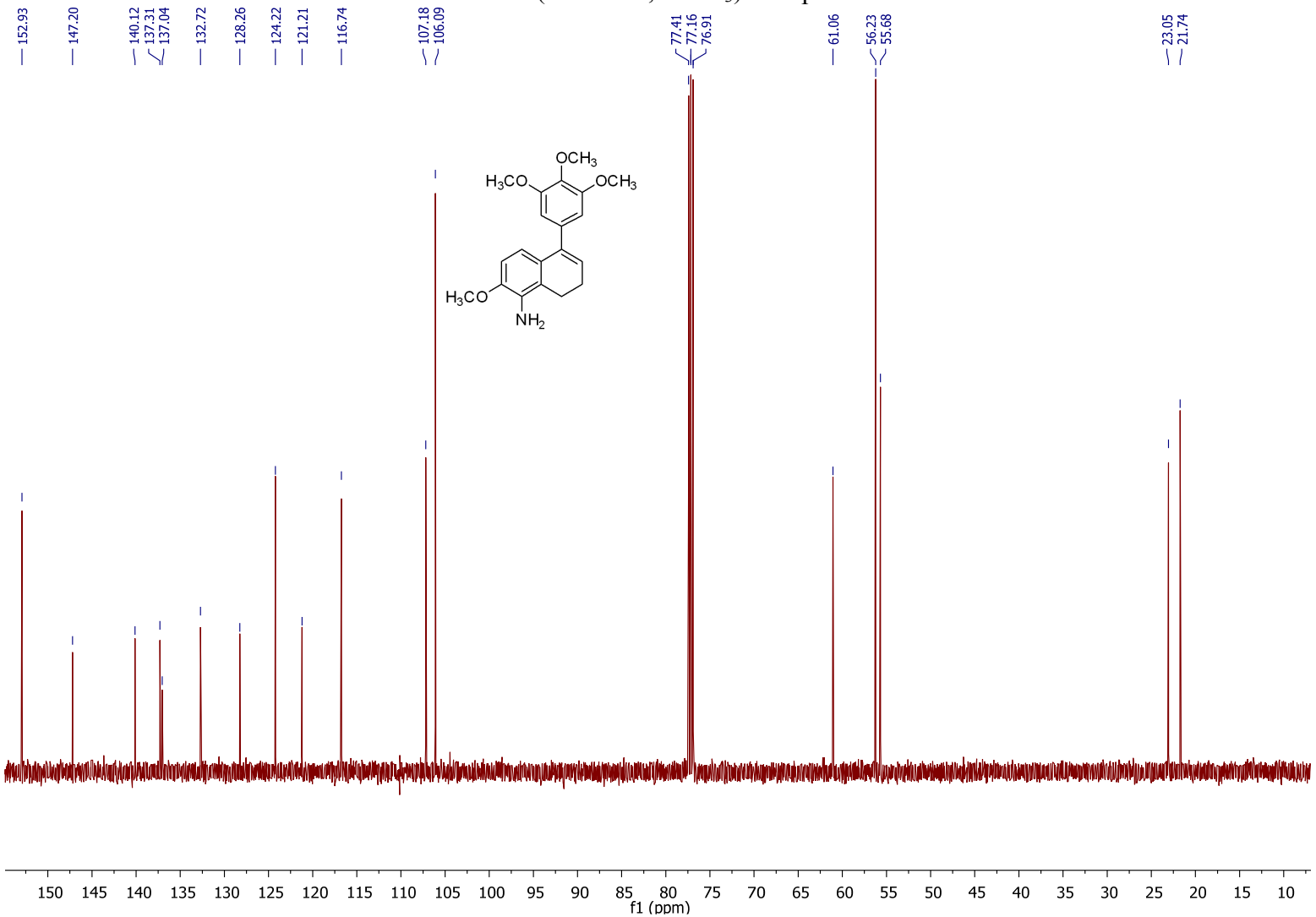

^{1}H NMR (500 MHz, $CDCl_3$) Compound 3

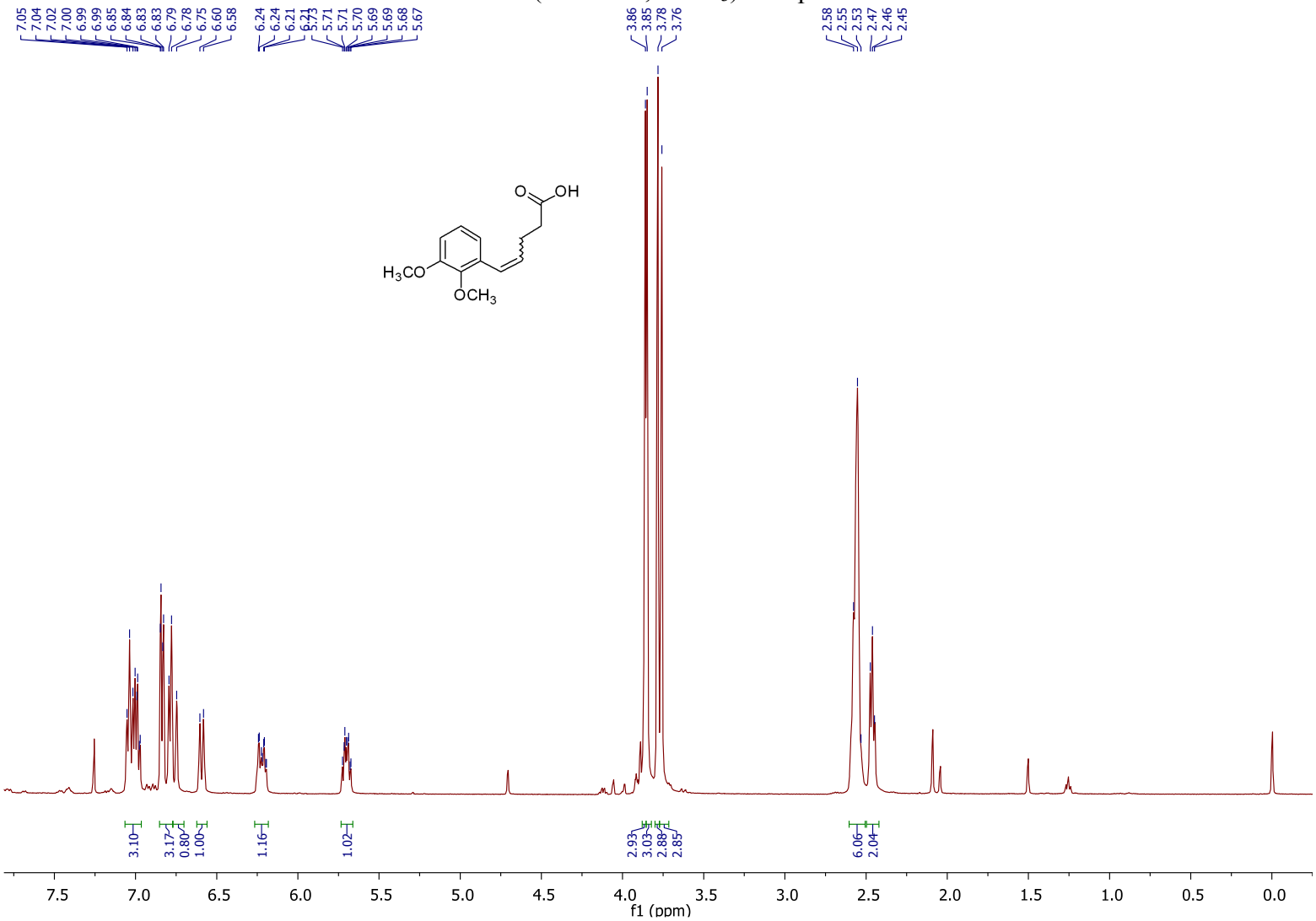

^{13}C NMR (125 MHz, $CDCl_3$) Compound 3

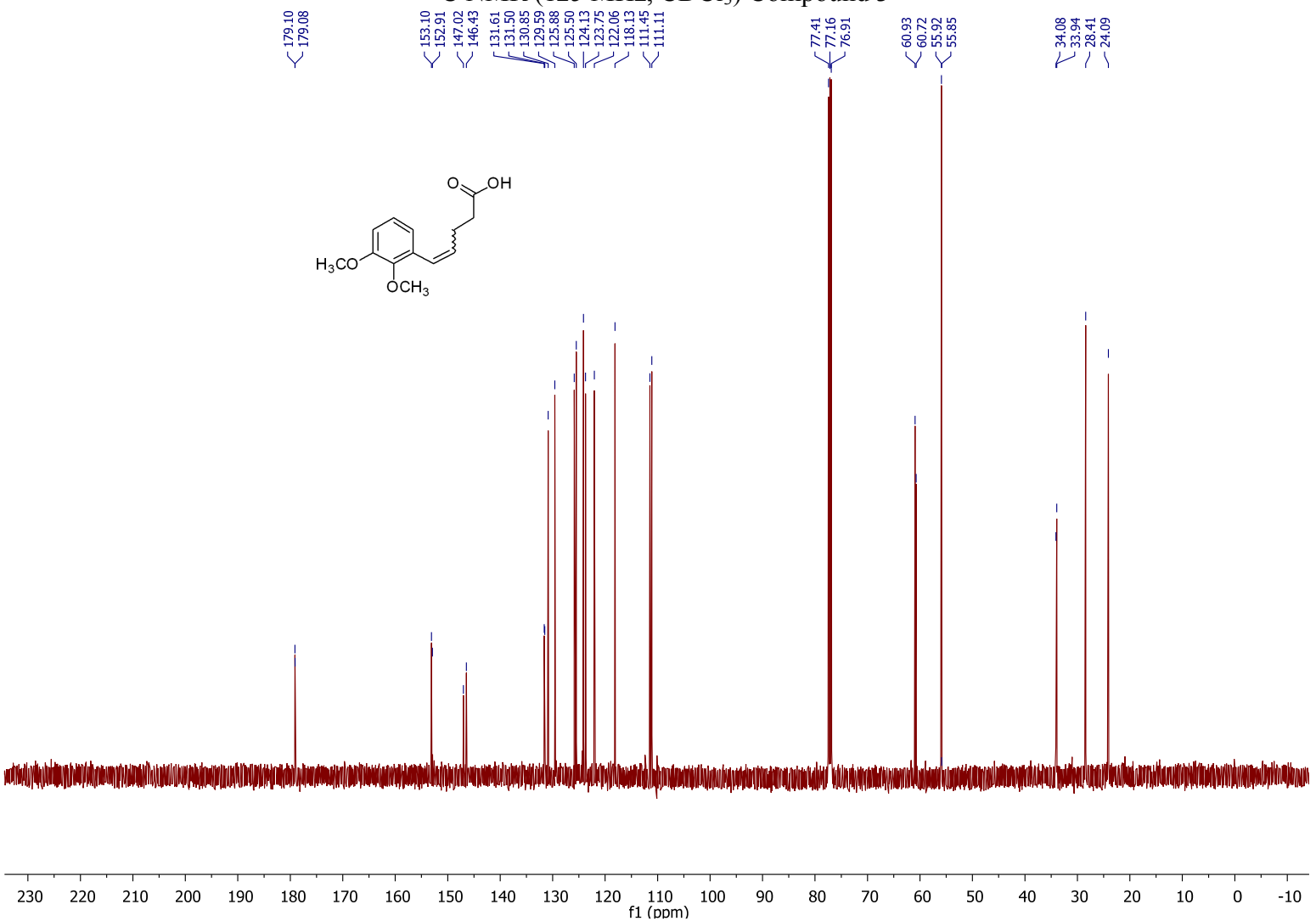

^{1}H NMR (500 MHz, $CDCl_3$) Compound 4

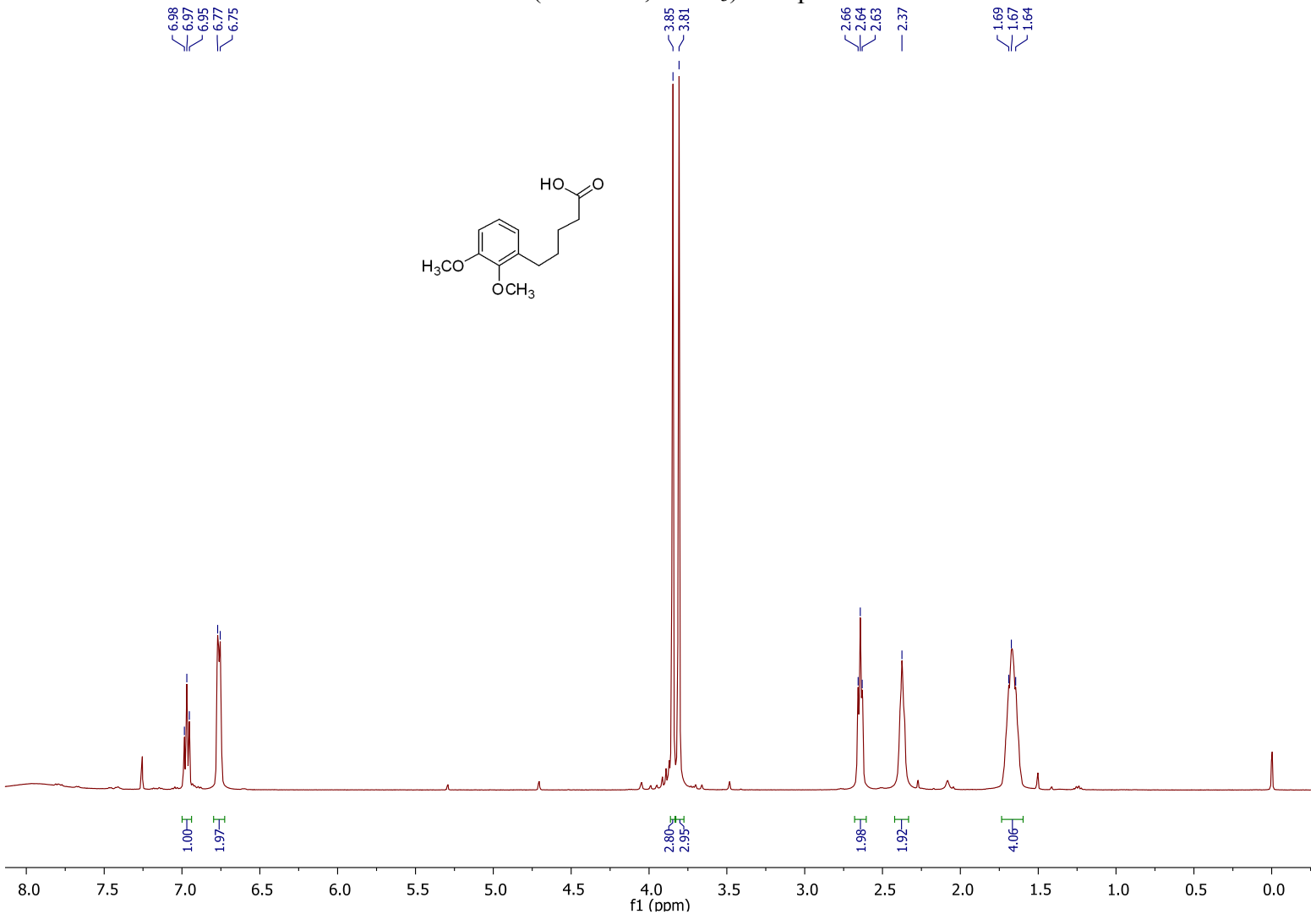

^{13}C NMR (125 MHz, $CDCl_3$) Compound 4

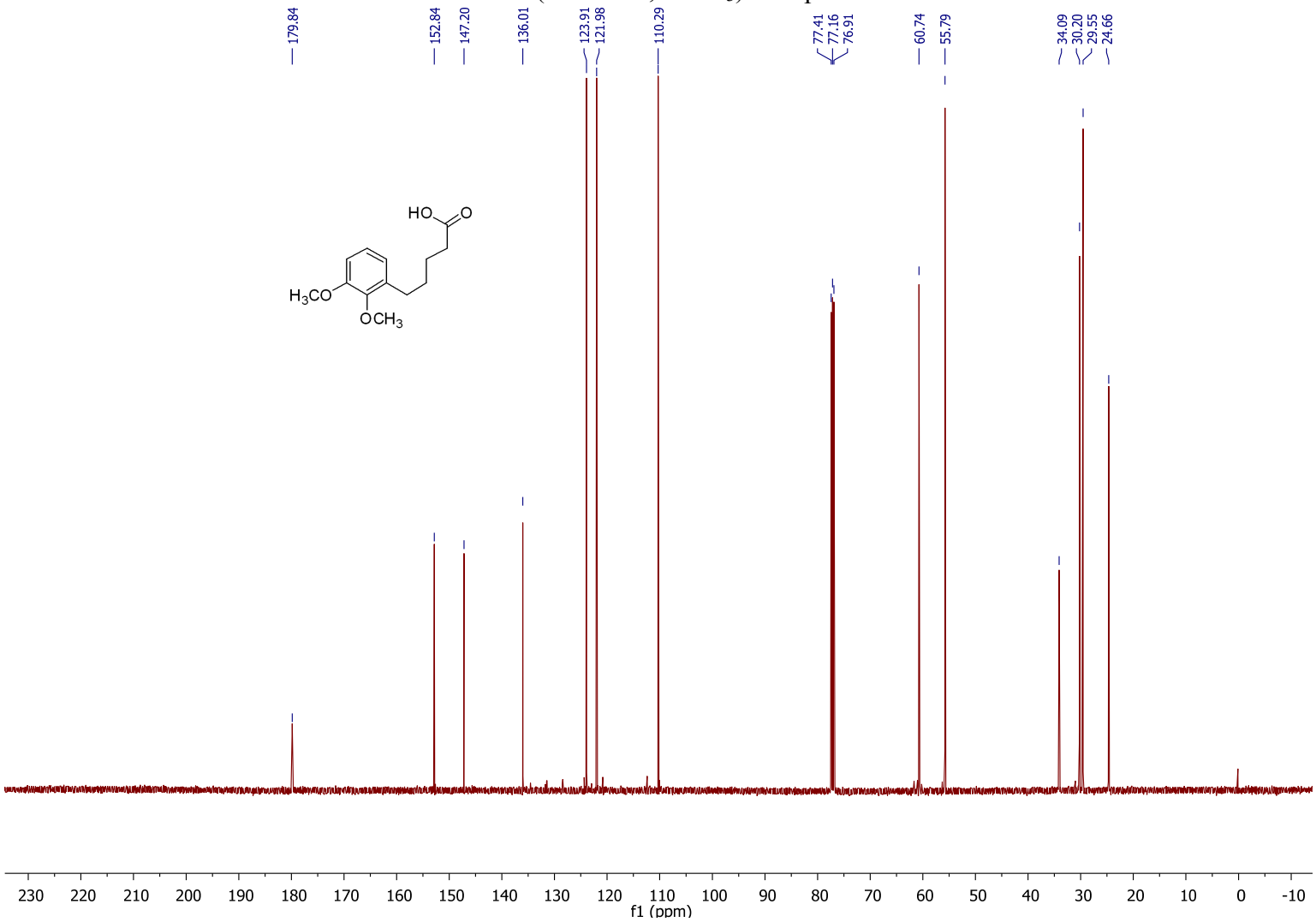

^{1}H NMR (500 MHz, $CDCl_3$) Compound 5

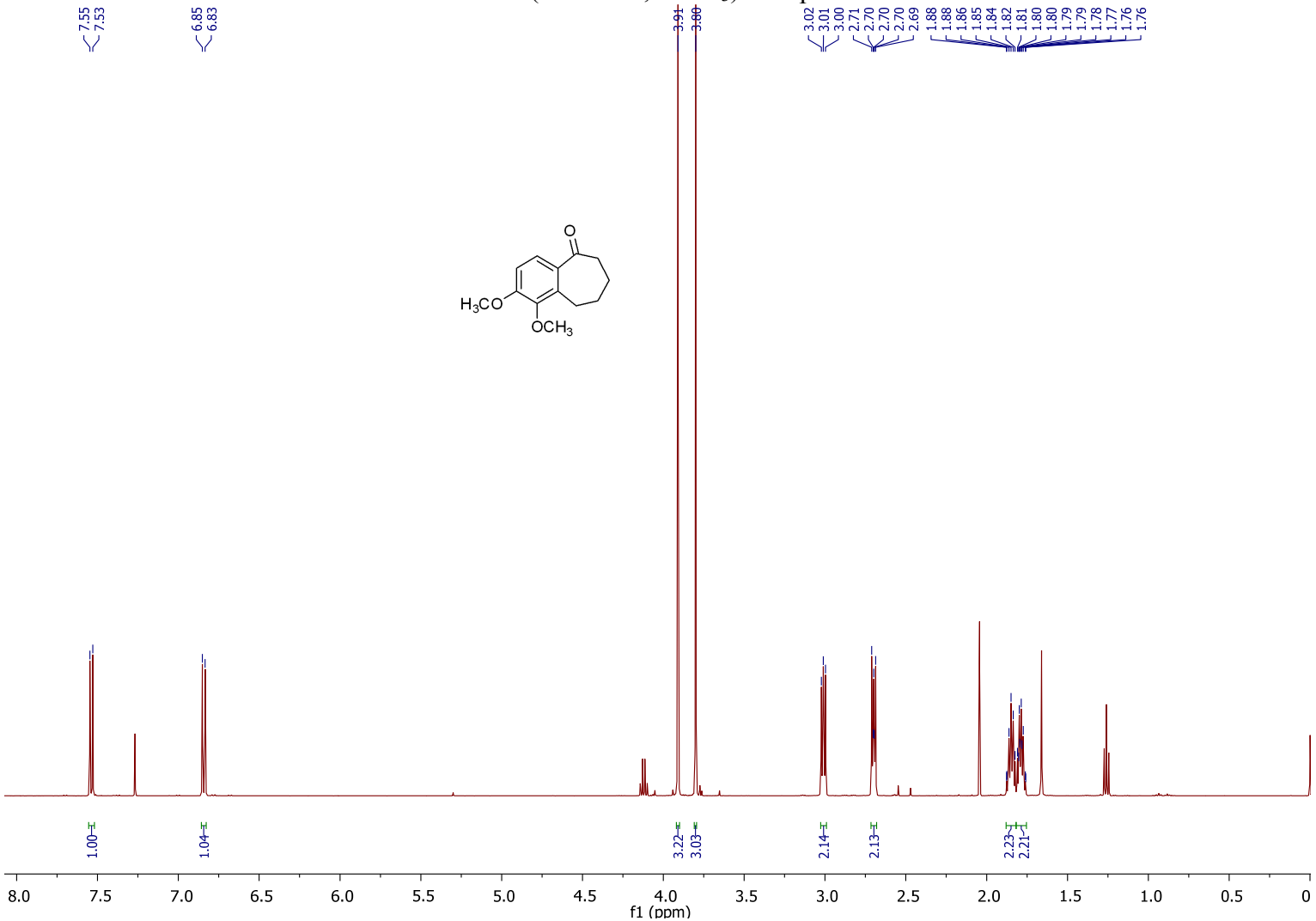

^{13}C NMR (125 MHz,$CDCl_3$) Compound 5

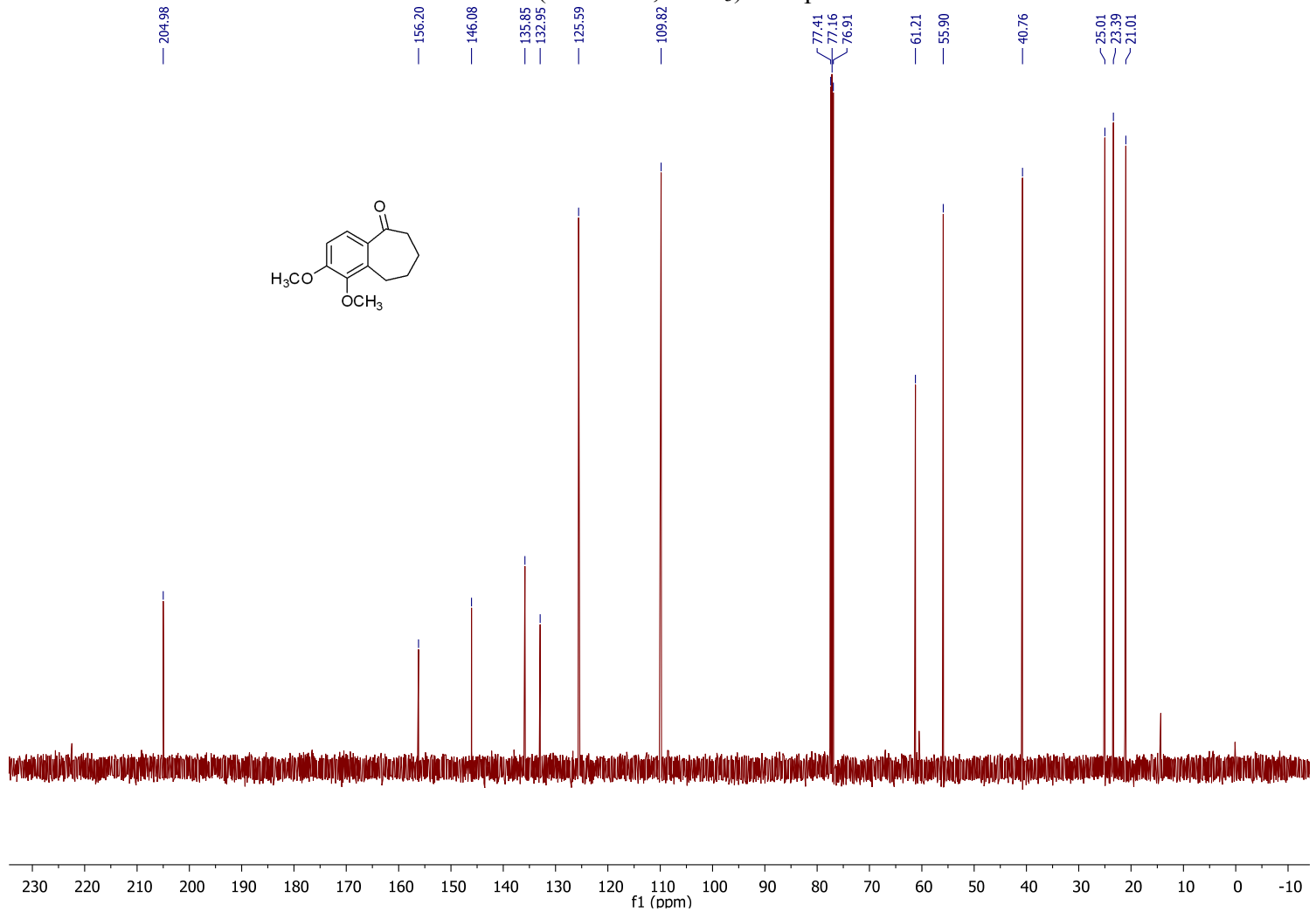

^{1}H NMR (500 MHz, $CDCl_3$) Compound 6

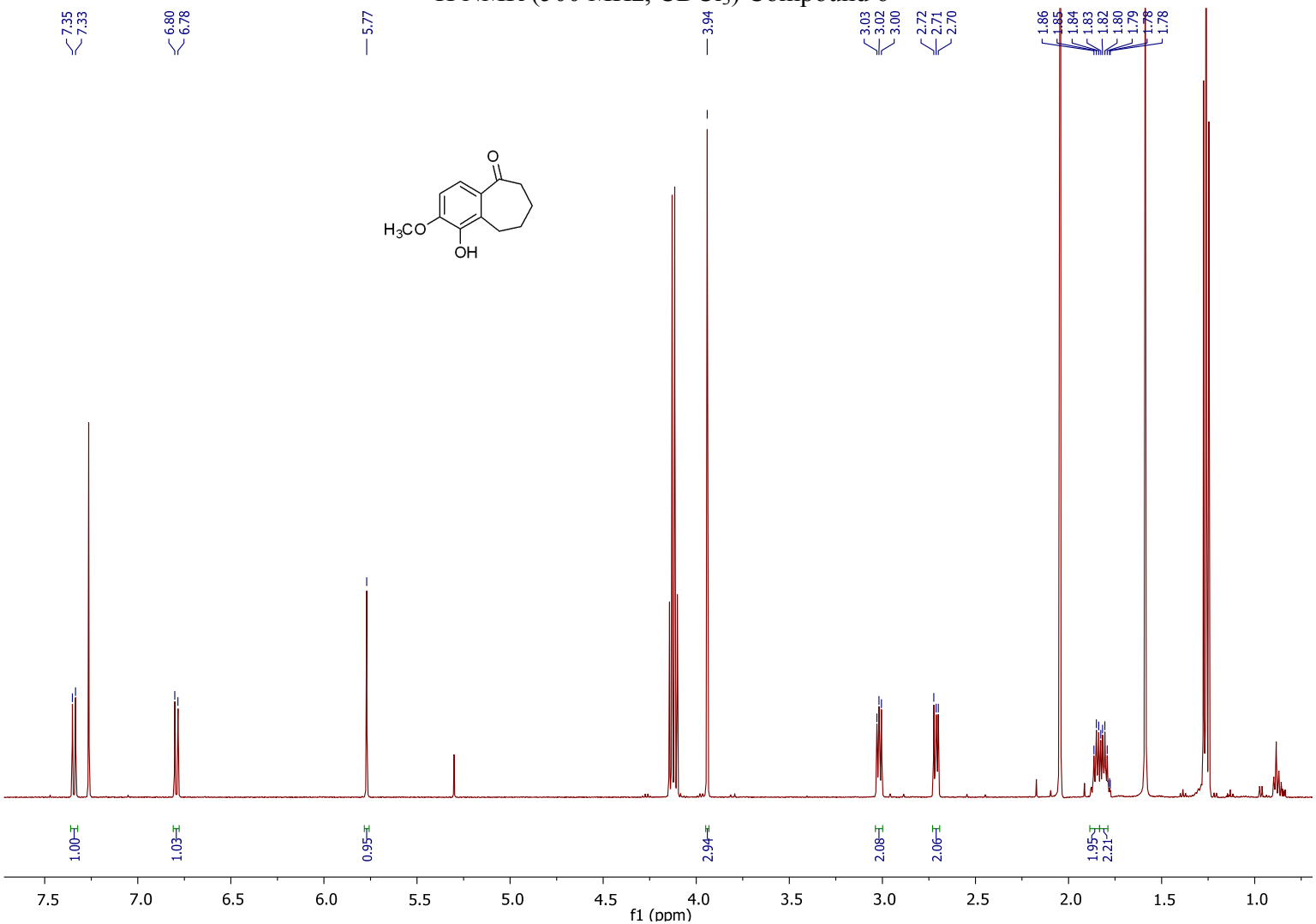

^{1}H NMR (500 MHz, $CDCl_3$) Compound 8

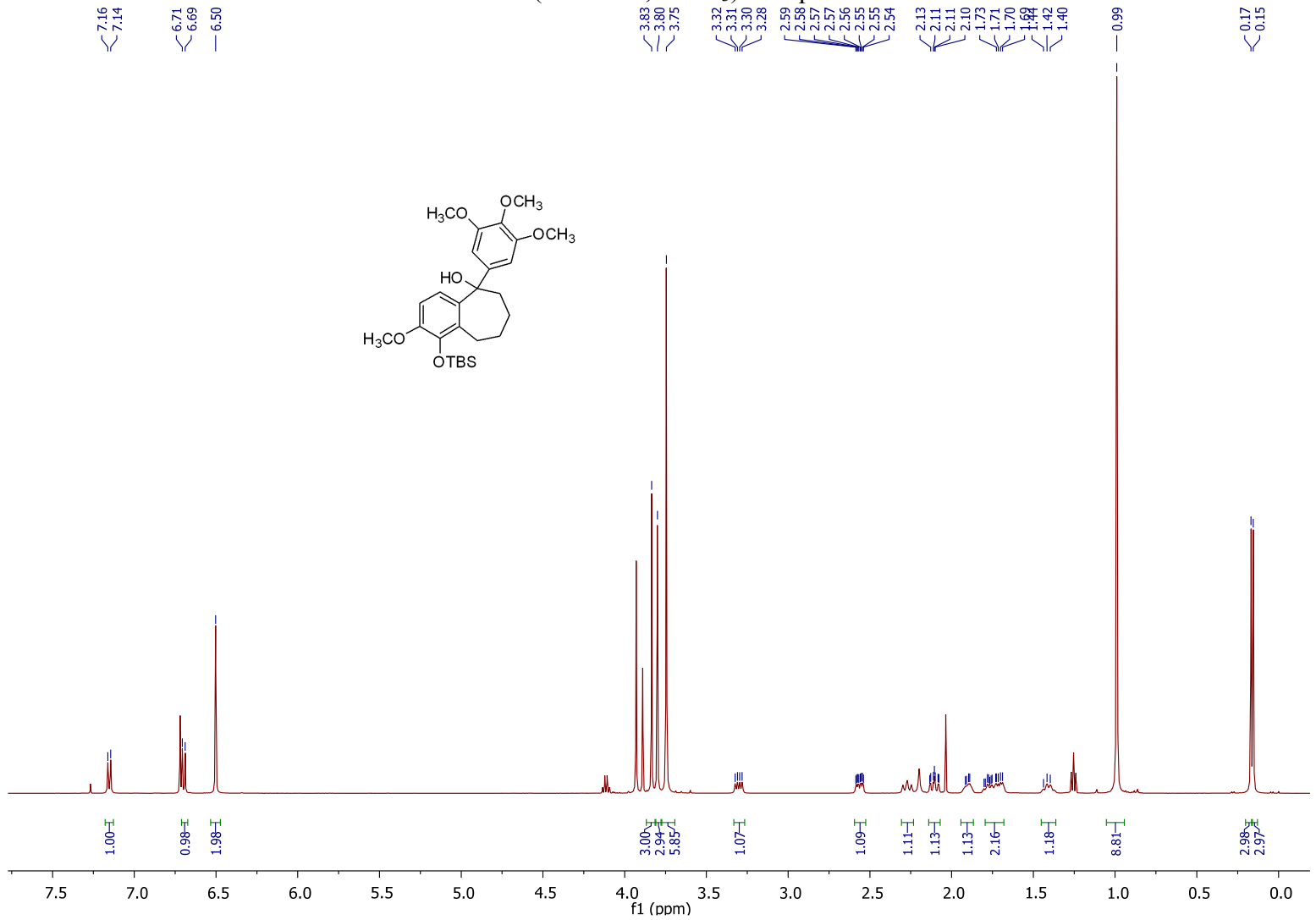

^{13}C NMR (125 MHz, $CDCl_3$) Compound 8

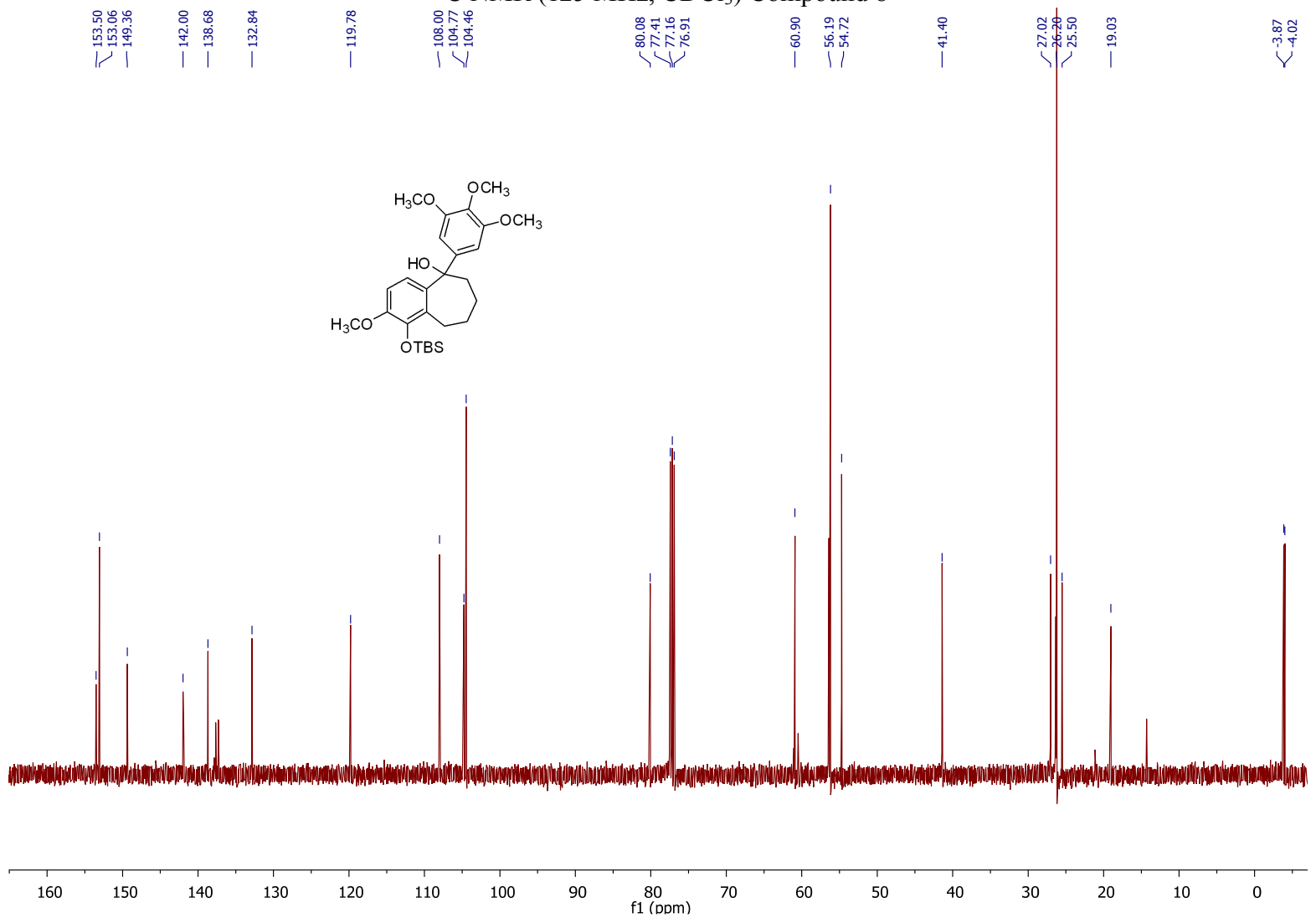

^{1}H NMR (500 MHz, $CDCl_3$) Compound 9

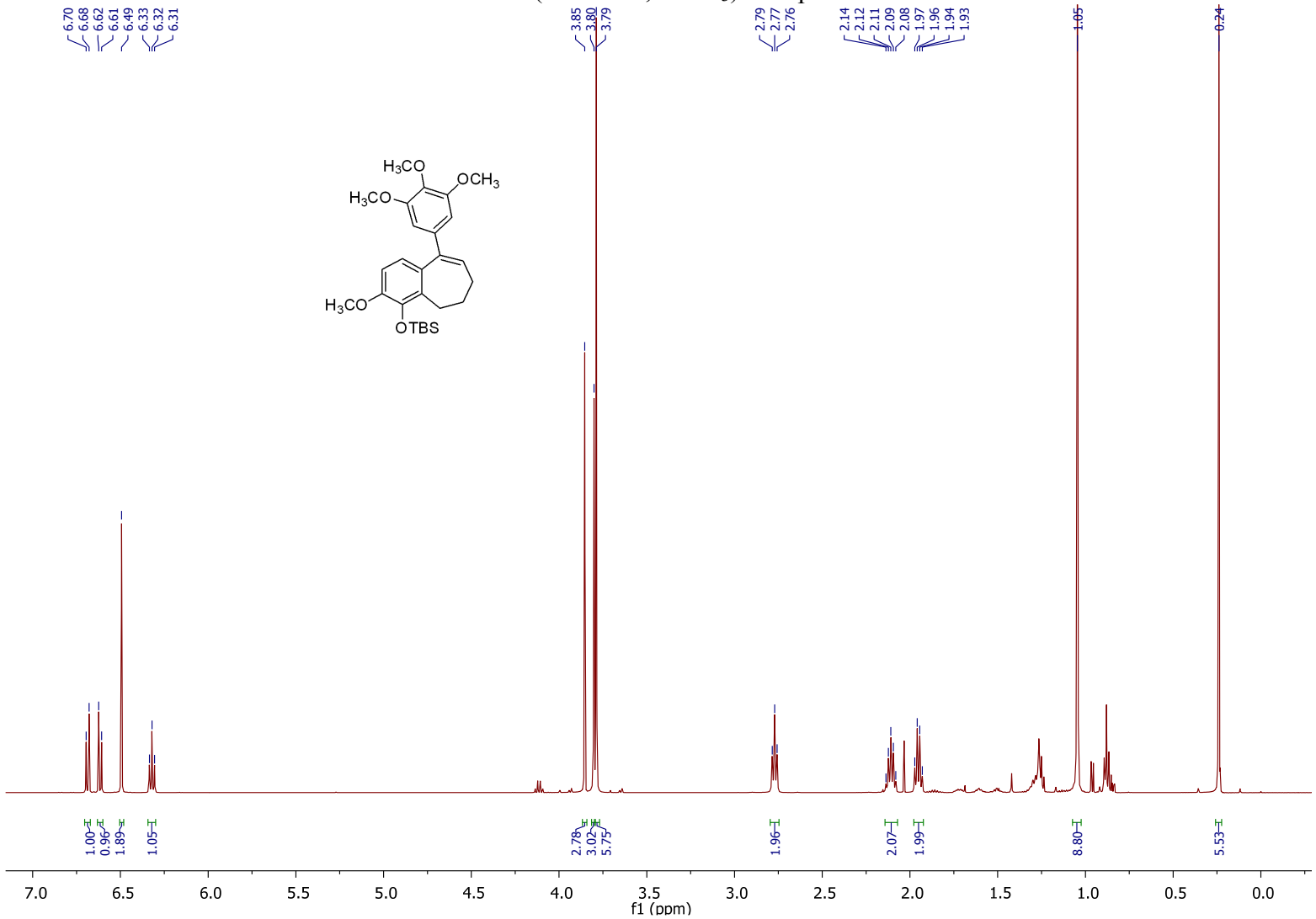

^{13}C NMR (125 MHz, $CDCl_3$) Compound 9

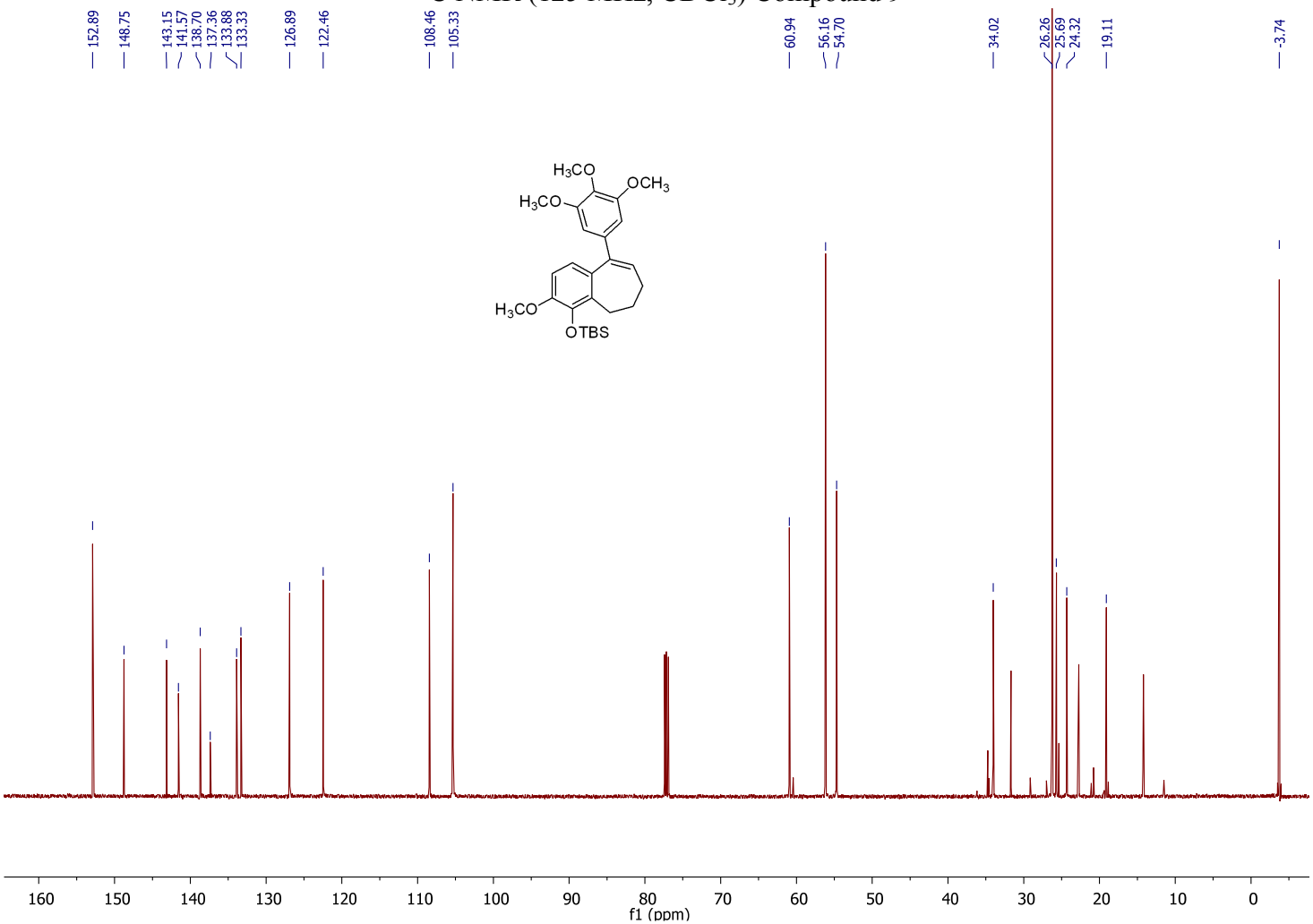

^{1}H NMR (500 MHz, $CDCl_3$) Compound 10

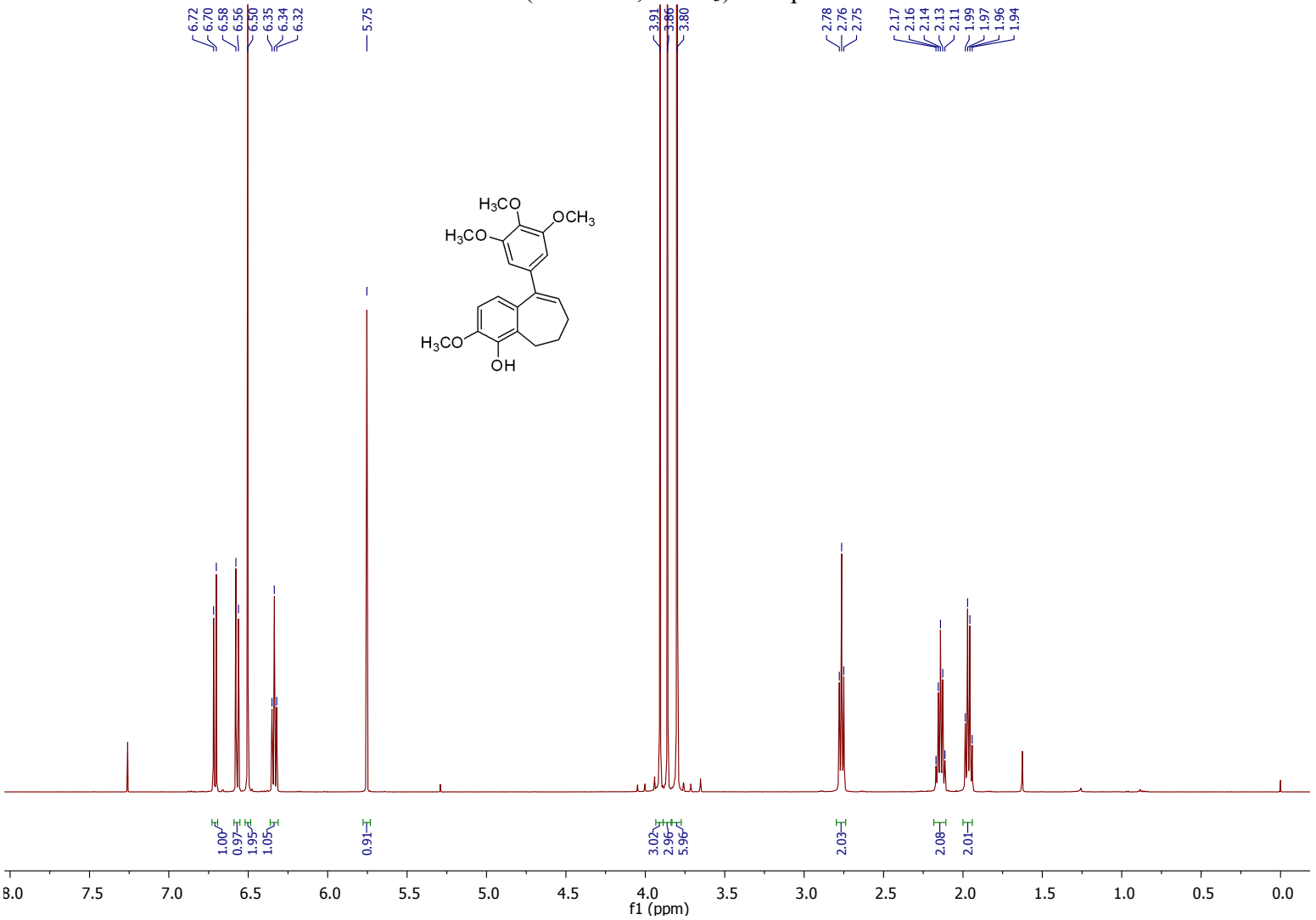

^{13}C NMR (125 MHz, $CDCl_3$) Compound 10

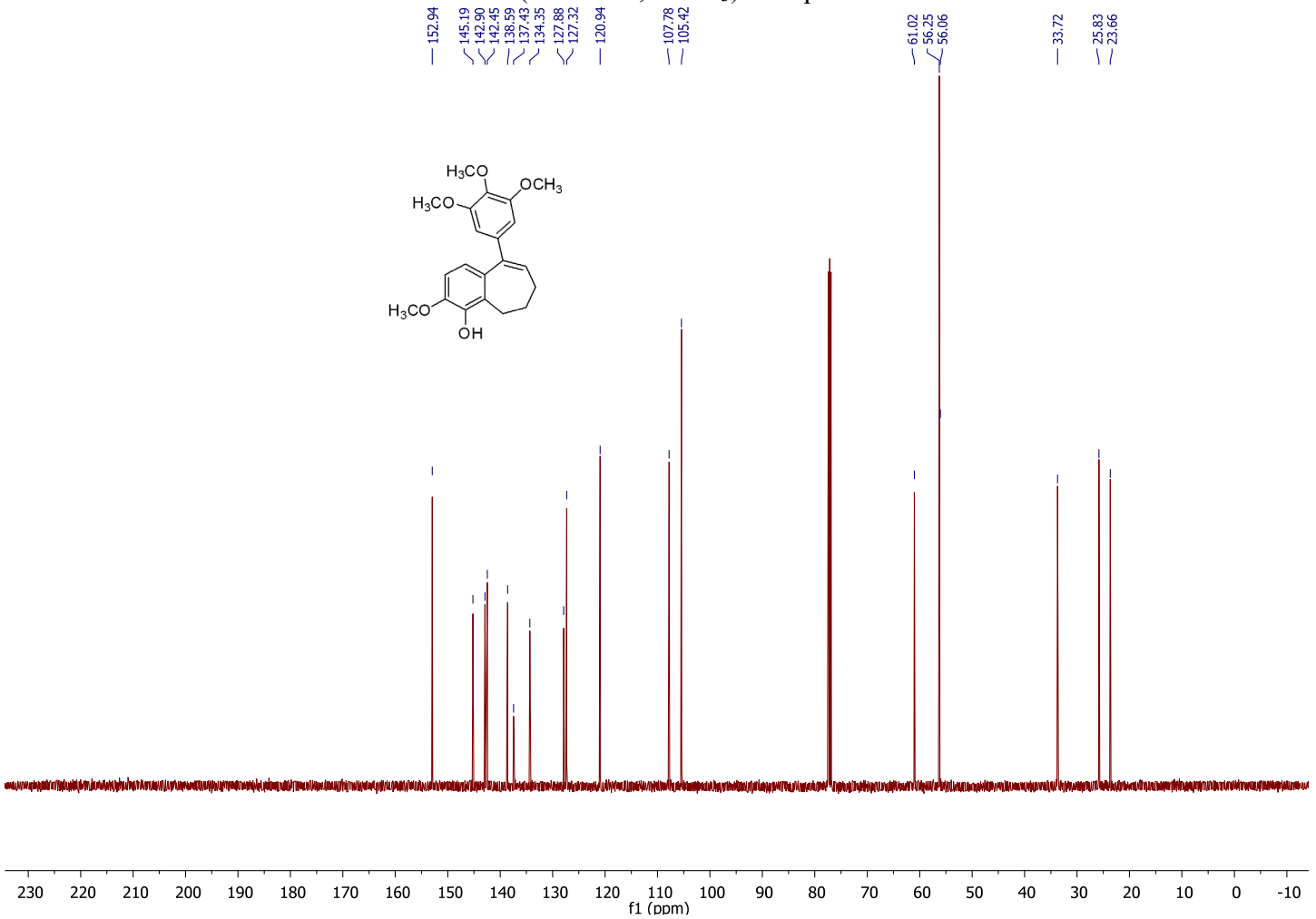

^{1}H NMR (500 MHz, DMSO) Compound 12

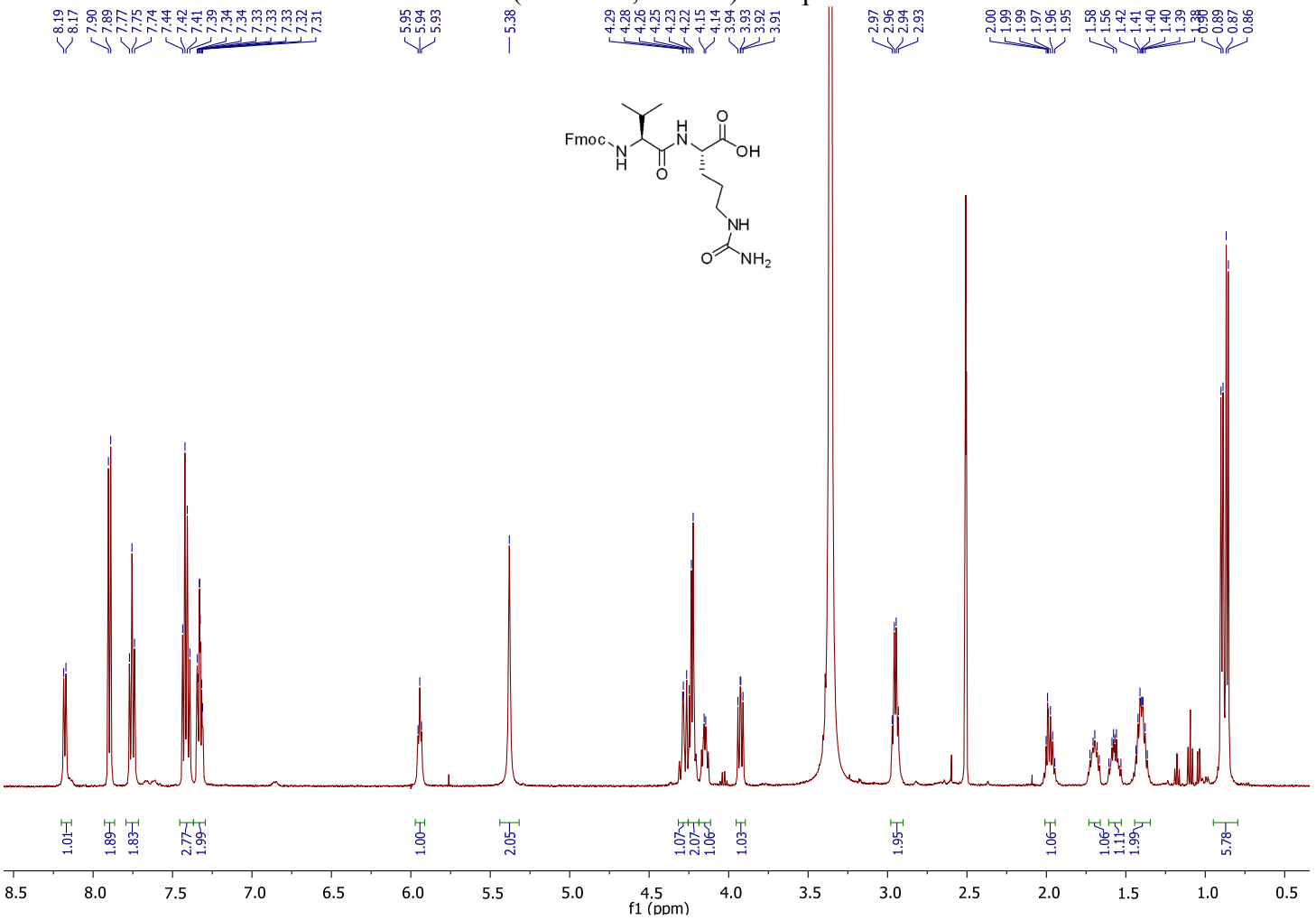

^{13}C NMR (125 MHz, DMSO) Compound 12

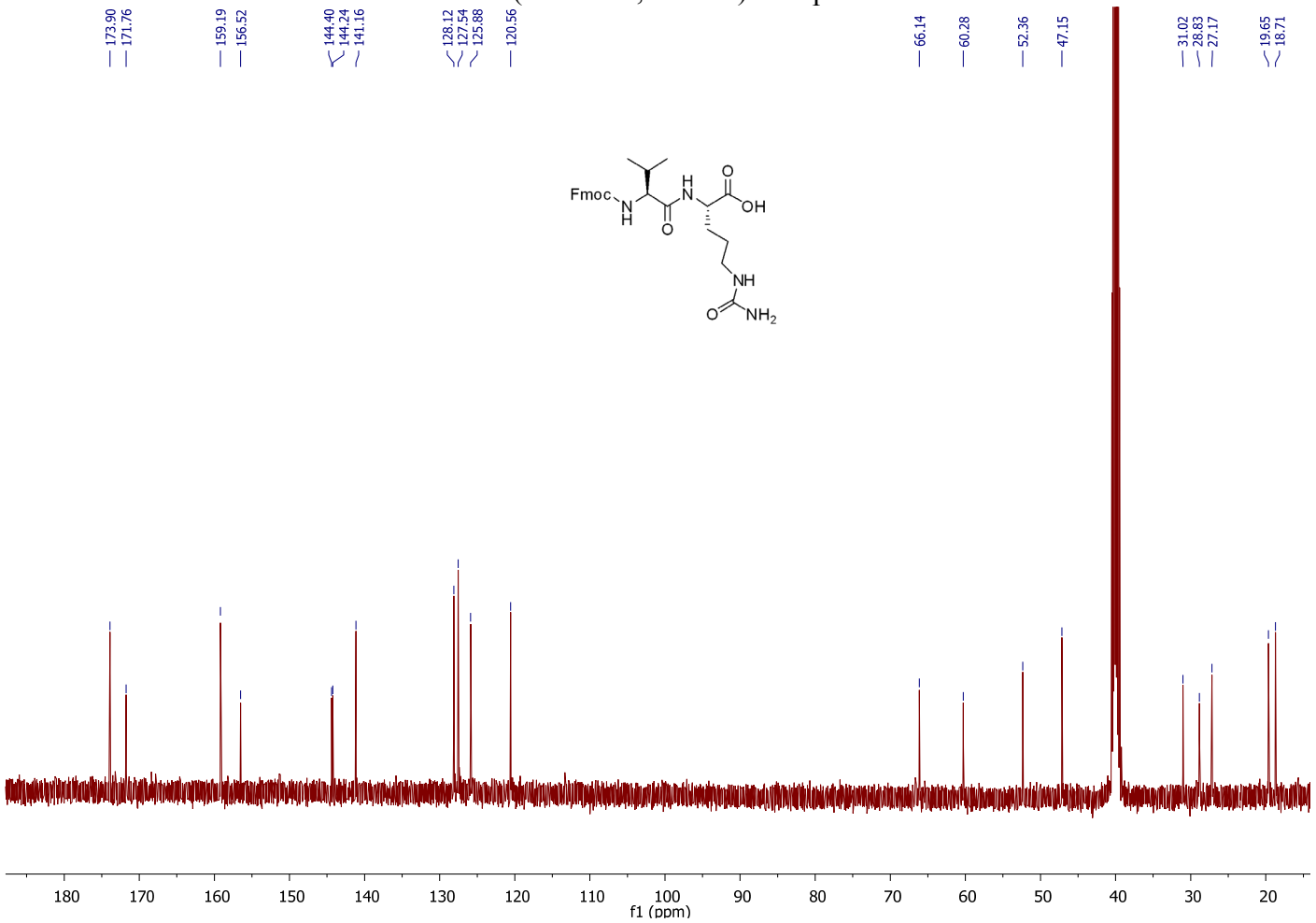

^{1}H NMR (500 MHz, DMSO) Compound 13

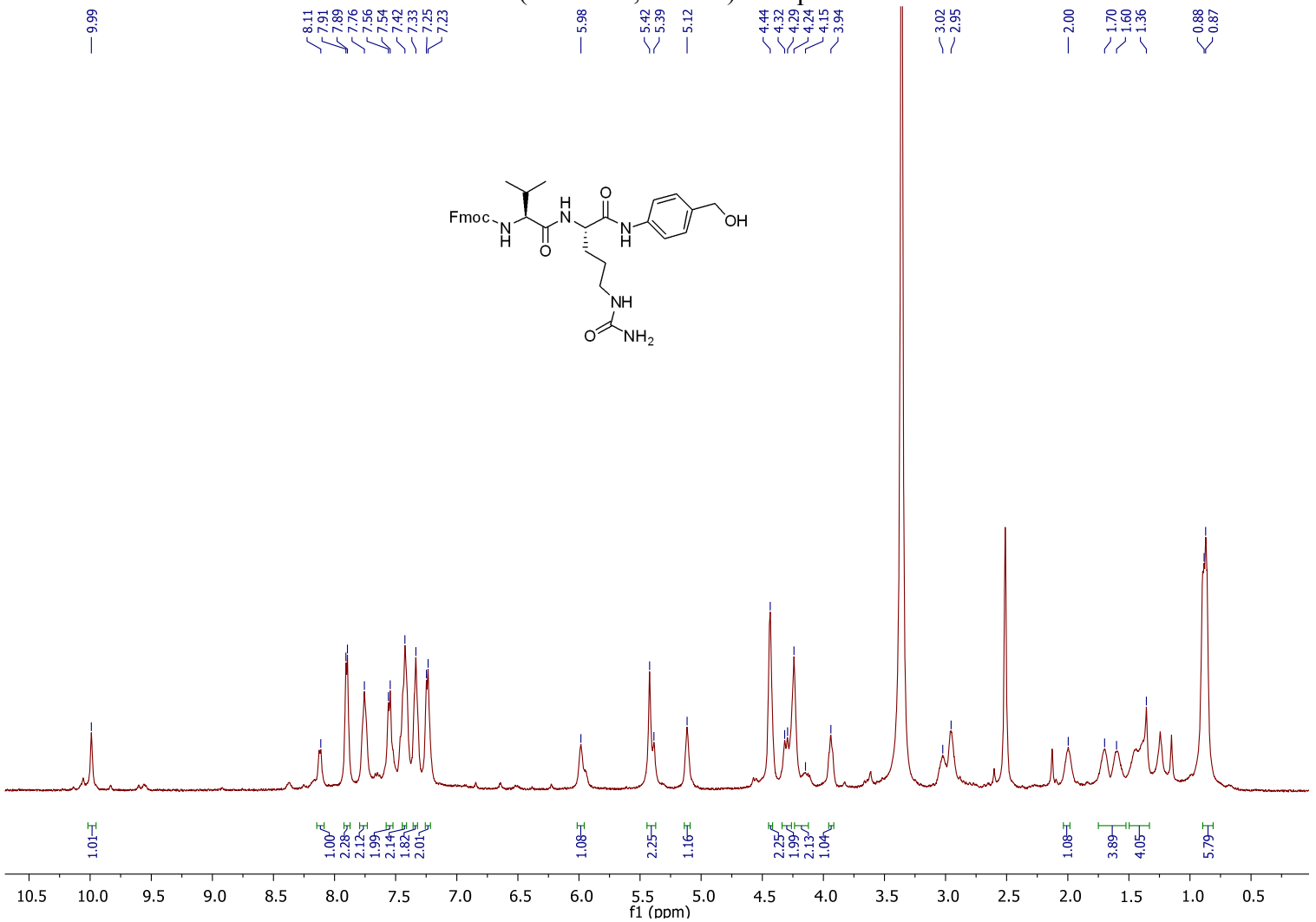

^{13}C NMR (125 MHz, DMSO) Compound 13

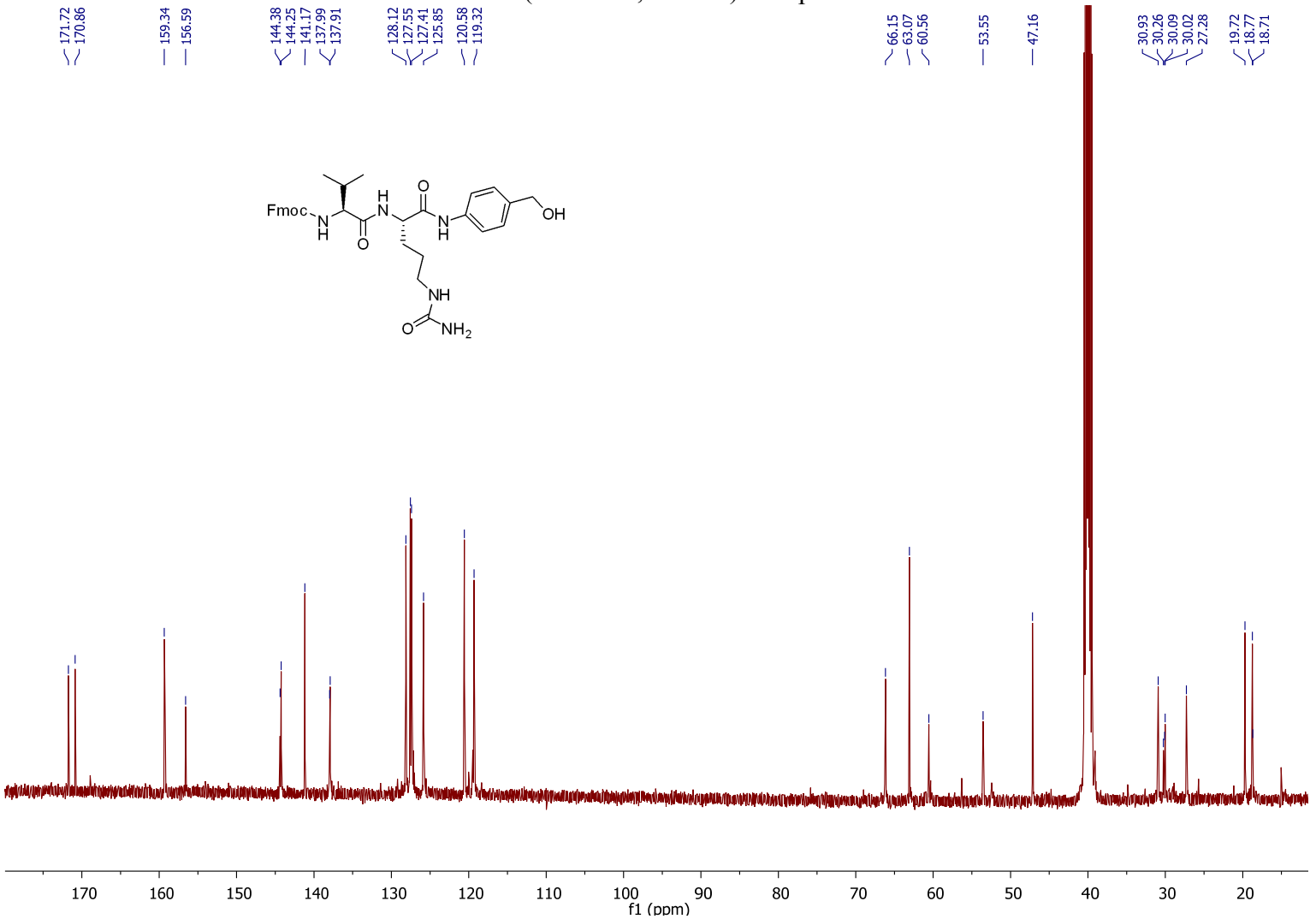

^{1}H NMR (500 MHz, DMSO) Compound 14

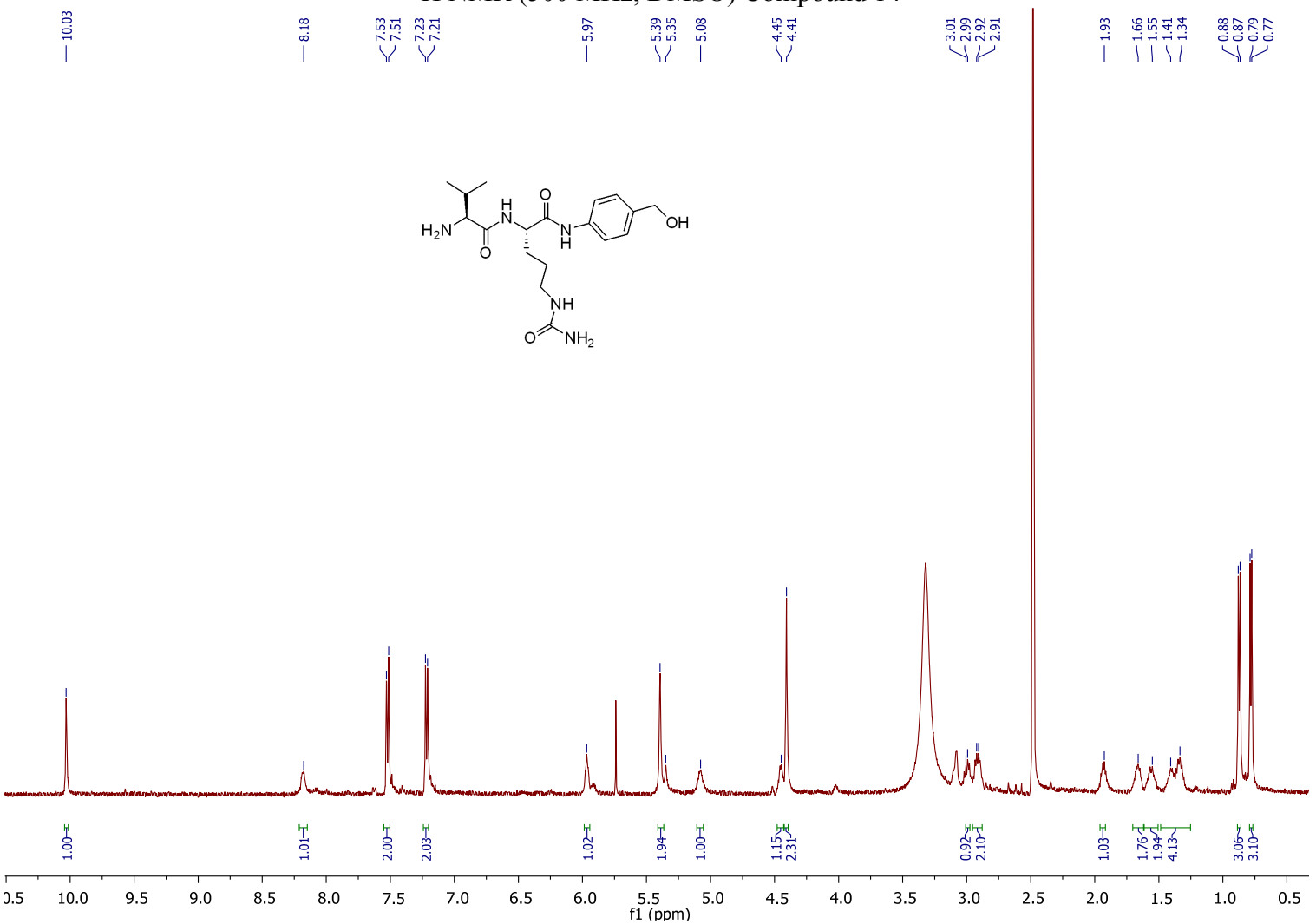

^{13}C NMR (125 MHz, DMSO) Compound 14

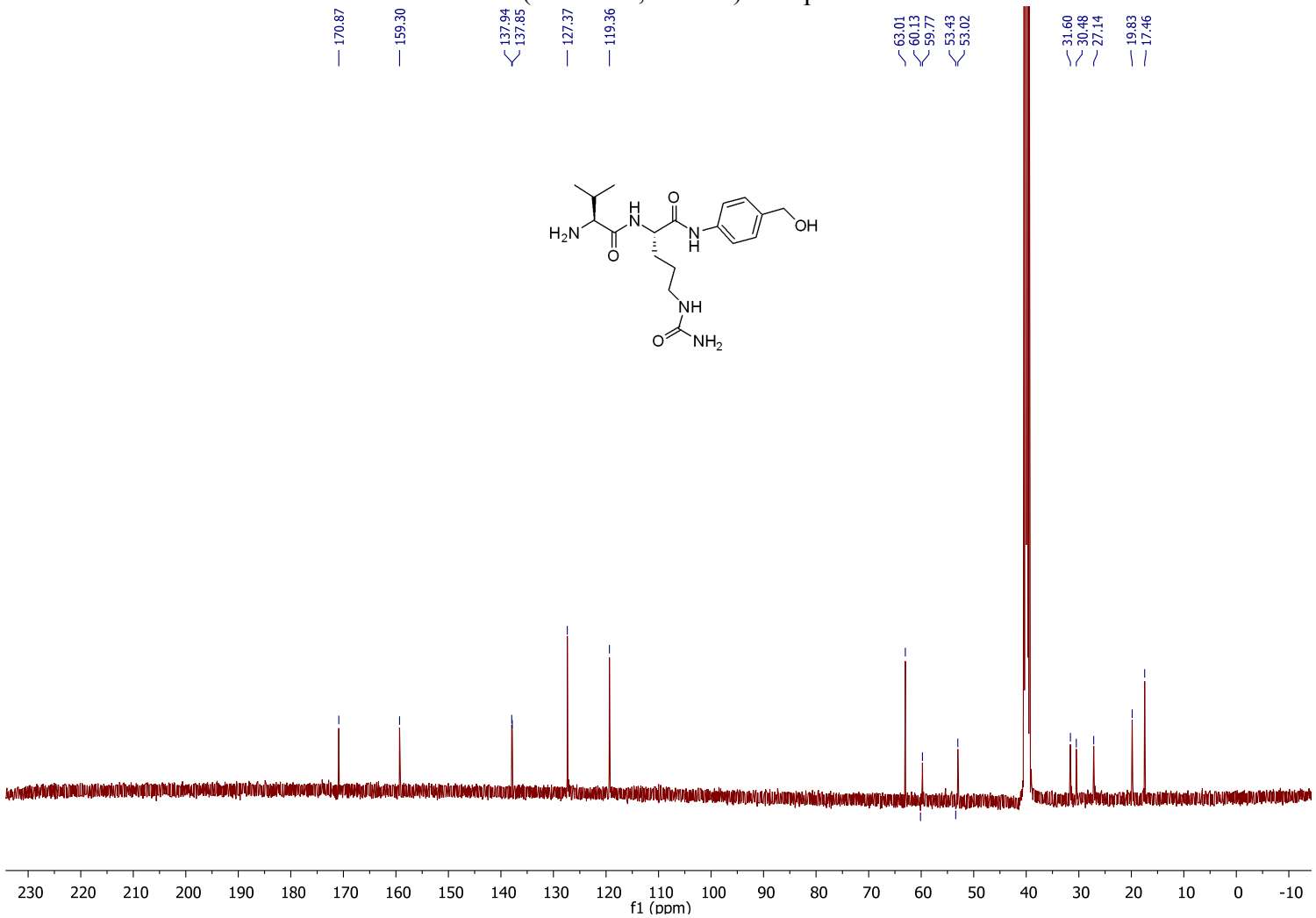

^{1}H NMR (500 MHz, $CDCl_3$) Compound 15

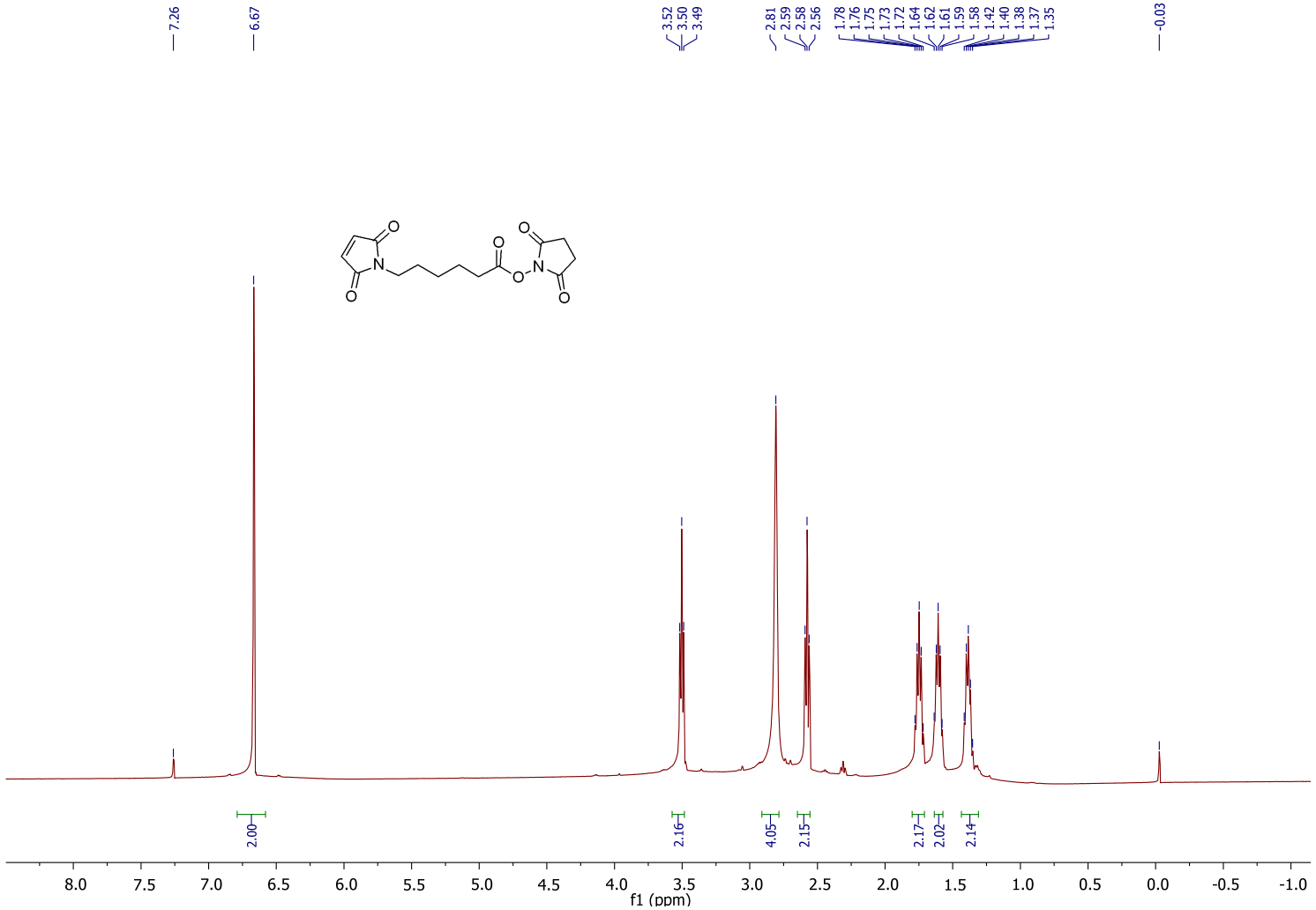

^{13}C NMR (125 MHz, $CDCl_3$) Compound 15

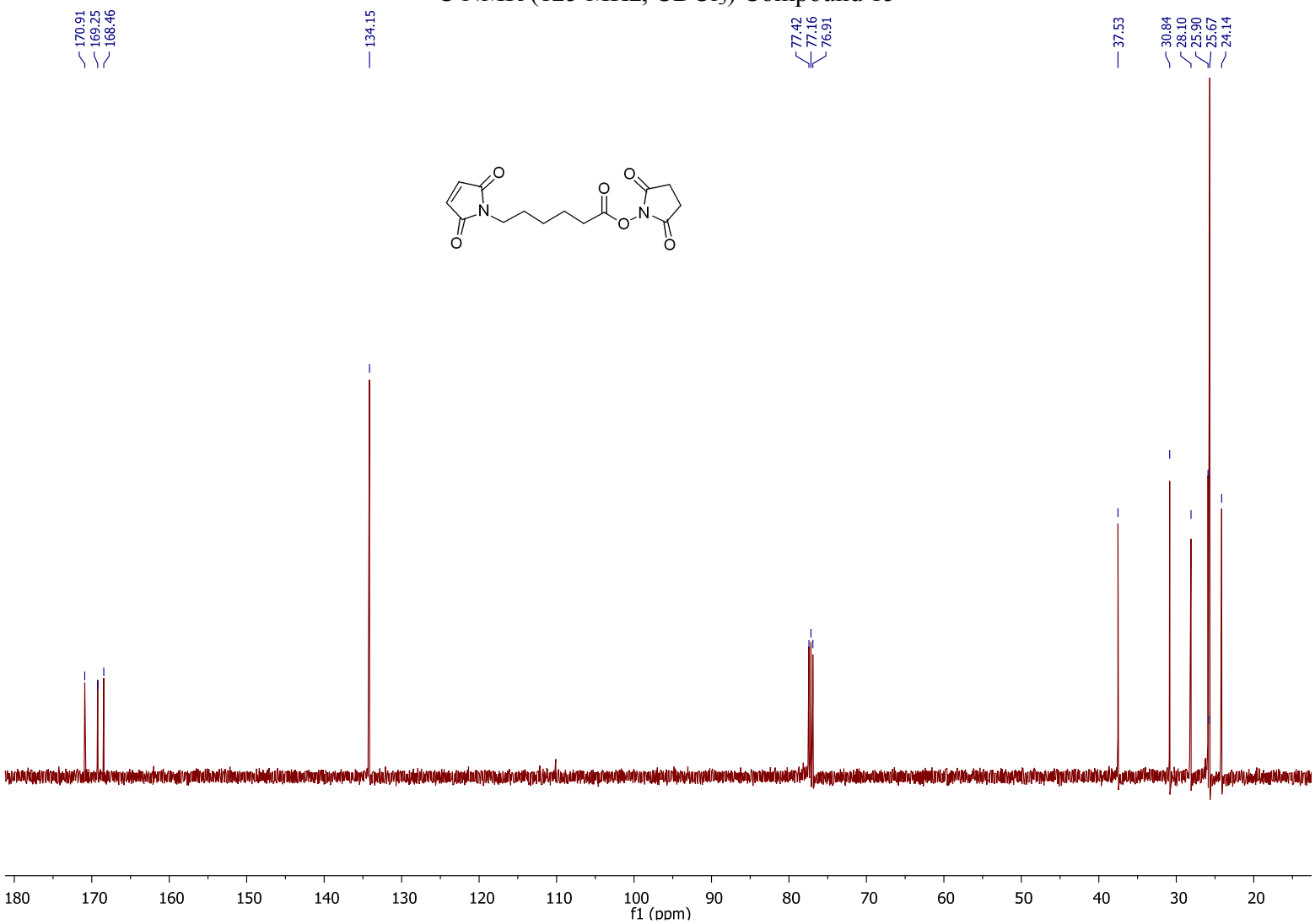

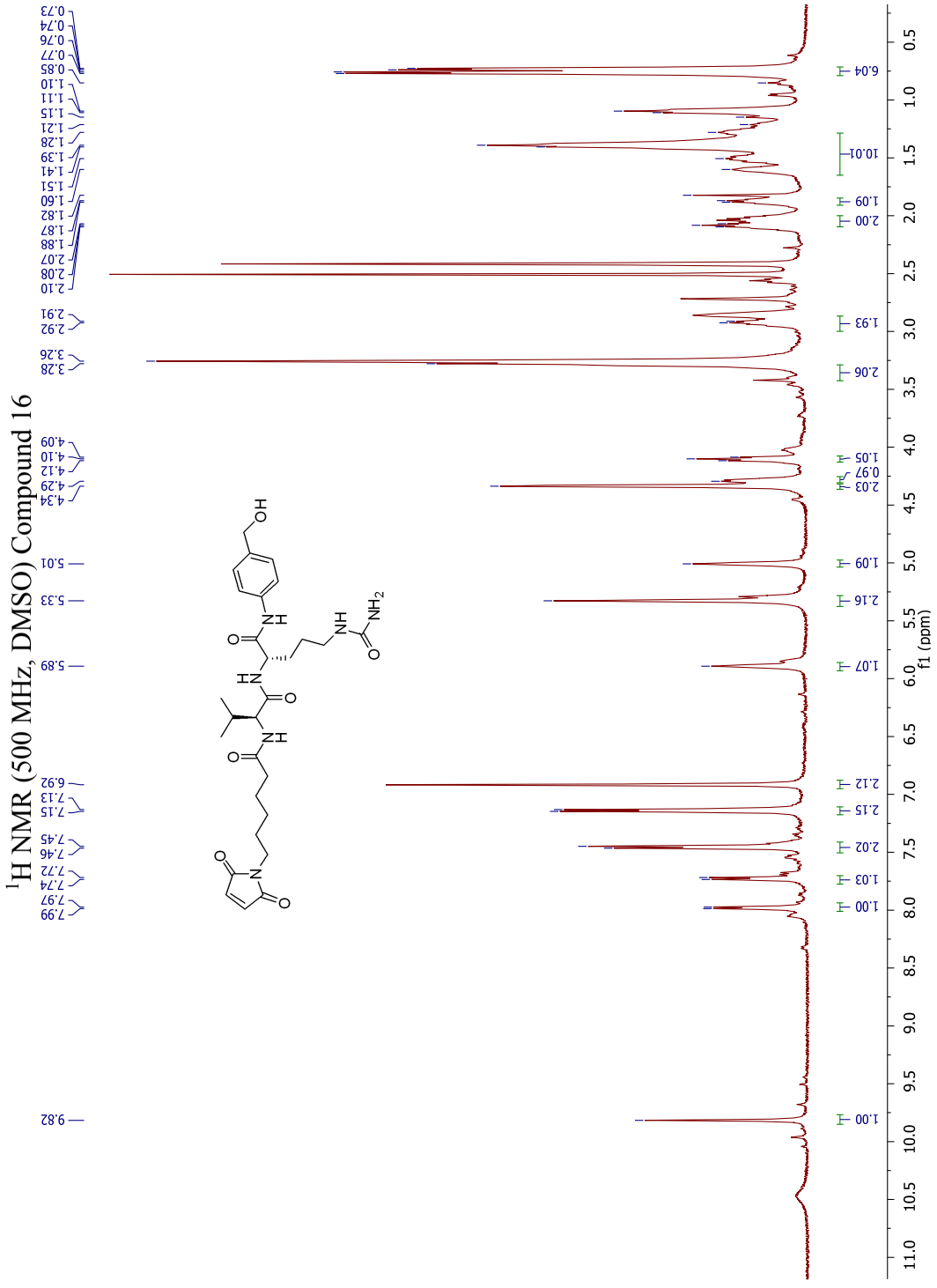
^{1}H NMR (500 MHz, DMSO) Compound 16
f1 (ppm)

^{13}C NMR (125 MHz, DMSO) Compound 16

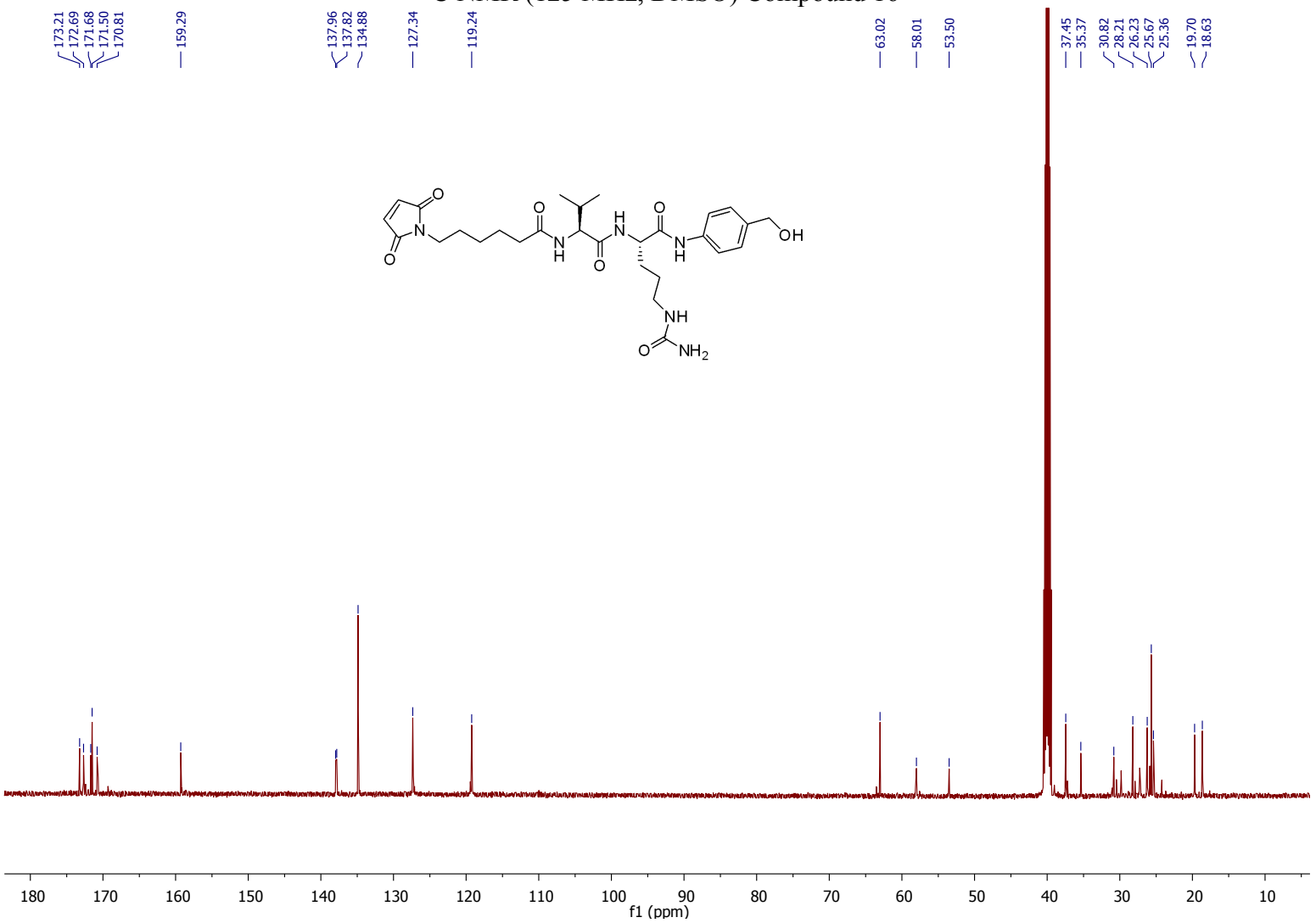

BIBLIOGRAPHY

(1) CDC - About United States Cancer Statistics - Cancer http://www.cdc.gov/cancer/npcr/about_uscs.htm (accessed Apr 11, 2014).

(2) Research, C. for D. E. and. Postmarket Drug Safety Information for Patients and Providers - Gleevec (Imatinib Mesylate) Questions and Answers http://www.fda.gov/Drugs/DrugSafety/PostmarketDrugSafetyInformationforPatientsandProviders/ucm110505.htm (accessed Apr 13, 2014).

(3) Trastuzumab — Mechanism of Action and Use. *N. Engl. J. Med.* **2007**, *357*, 1664–1666.

(4) Tozer, G. M.; Kanthou, C.; Baguley, B. C. Disrupting Tumour Blood Vessels. *Nat. Rev. Cancer* **2005**, *5*, 423–435.

(5) Siemann, D. W. The Unique Characteristics of Tumor Vasculature and Preclinical Evidence for Its Selective Disruption by Tumor-Vascular Disrupting Agents. *Cancer Treat. Rev.* **2011**, *37*, 63–74.

(6) Ruoslahti, E. Specialization Of Tumour Vasculature. *Nat. Rev. Cancer* **2002**, *2*, 83–90.

(7) Zolot, R. S.; Basu, S.; Million, R. P. Antibody–drug Conjugates. *Nat. Rev. Drug Discov.* **2013**, *12*, 259–260.

(8) Stack, G. D.; Walsh, J. J. Optimising the Delivery of Tubulin Targeting Agents through Antibody Conjugation. *Pharm. Res.* **2012**, *29*, 2972–2984.

(9) Schnell, O.; Krebs, B.; Wagner, E.; Romagna, A.; Beer, A. J.; Grau, S. J.; Thon, N.; Goetz, C.; Kretzschmar, H. A.; Tonn, J.-C.; Goldbrunner, R. H. Expression of Integrin $A_v B_3$ in Gliomas Correlates with Tumor Grade and Is Not Restricted to Tumor Vasculature. *Brain Pathol.* **2008**, *18*, 378–386.

(10) Denekamp, J. Endothelial Cell Proliferation as a Novel Approach to Targeting Tumour Therapy. *Br. J. Cancer* **1982**, *45*, 136–139.

(11) Thorpe, P. E. Vascular Targeting Agents as Cancer Therapeutics. *Clin. Cancer Res.* **2004**, *10*, 415–427.

(12) Hill, S. A.; Lonergan, S. J.; Denekamp, J.; Chaplin, D. J. The Effect of Vinca Alkaloids on Tumour Blood Flow. *Adv. Exp. Med. Biol.* **1994**, *345*, 417–422.

(13) Monk, K. A.; Siles, R.; Hadimani, M. B.; Mugabe, B. E.; Ackley, J. F.; Studerus, S. W.; Edvardsen, K.; Trawick, M. L.; Garner, C. M.; Rhodes, M. R.; Pettit, G. R.; Pinney, K. G. Design, Synthesis, and Biological Evaluation of Combretastatin Nitrogen-Containing Derivatives as Inhibitors of Tubulin Assembly and Vascular Disrupting Agents. *Bioorg. Med. Chem.* **2006**, *14*, 3231–3244.

(14) Sriram, M.; Hall, J. J.; Grohmann, N. C.; Strecker, T. E.; Wootton, T.; Franken, A.; Trawick, M. L.; Pinney, K. G. Design, Synthesis and Biological Evaluation of Dihydronaphthalene and Benzosuberene Analogs of the Combretastatins as Inhibitors of Tubulin Polymerization in Cancer Chemotherapy. *Bioorg. Med. Chem.* **2008**, *16*, 8161–8171.

(15) Mason, R. P.; Zhao, D.; Liu, L.; Trawick, M. L.; Pinney, K. G. A Perspective on Vascular Disrupting Agents That Interact with Tubulin: Preclinical Tumor Imaging and Biological Assessment. *Integr. Biol. Quant. Biosci. Nano Macro* **2011**, *3*, 375–387.

(16) Siles, R.; Ackley, J. F.; Hadimani, M. B.; Hall, J. J.; Mugabe, B. E.; Guddneppanavar, R.; Monk, K. A.; Chapuis, J.-C.; Pettit, G. R.; Chaplin, D. J.; Edvardsen, K.; Trawick, M. L.; Garner, C. M.; Pinney, K. G. Combretastatin Dinitrogen-Substituted Stilbene Analogues as Tubulin-Binding and Vascular-Disrupting Agents. *J. Nat. Prod.* **2008**, *71*, 313–320.

(17) Chen, Z.; O'Donnell, C. J.; Maderna, A. Synthesis of 3-Methoxy-9-(3,4,5-Trimethoxyphenyl)-6,7-Dihydro-5H-benzo[7]annulen-4-Ol, a Potent Antineoplastic Benzosuberene Derivative for Anti-Cancer Chemotherapy. *Tetrahedron Lett.* **2012**, *53*, 64–66.

(18) Sriram, M. *Design, Synthesis, Biochemical and Biological Evaluation of Benzocyclic and Enediyne Analogs of Combretastatins as Potential Tubulin Binding Ligands in the Treatment of Cancer*; Ph.D. Dissertation, Baylor University, Waco, TX 2000.

(19) Tanpure, R. P.; George, C. S.; Strecker, T. E.; Devkota, L.; Tidmore, J. K.; Lin, C.-M.; Herdman, C. A.; MacDonough, M. T.; Sriram, M.; Chaplin, D. J.; Trawick, M. L.; Pinney, K. G. Synthesis of Structurally Diverse Benzosuberene Analogues and Their Biological Evaluation as Anti-Cancer Agents. *Bioorg. Med. Chem.* **2013**, *21*, 8019–8032.

(20) Chen, Z.; Dorsey, J.; Garner, C.; Ghatak, A.; Hadimani, M.; Kessler, J.; Mocharla, V.; Pinney, K. Tubulin Binding Ligands and Corresponding Prodrug Constructs. US20020055643 A1, May 9, 2002.

(21) Denny, W. Role of Hypoxia Activated Prodrugs. *The Lancet* **2000**, *1*, 25–29.

(22) Wilson, W. R.; Hay, M. P. Targeting Hypoxia in Cancer Therapy. *Nat. Rev. Cancer* **2011**, *11*, 393–410.

(23) Chen, Y.; Hu, L. Design of Anticancer Prodrugs for Reductive Activation. *Med. Res. Rev.* **2009**, *29*, 29–64.

(24) Thomson, P.; Naylor, M. A.; Everett, S. A.; Stratford, M. R. L.; Lewis, G.; Hill, S.; Patel, K. B.; Wardman, P.; Davis, P. D. Synthesis and Biological Properties of Bioreductively Targeted Nitrothienyl Prodrugs of Combretastatin A-4. *Mol. Cancer Ther.* **2006**, *5*, 2886–2894.

(25) Chen, Z.; Maderna, A.; Sukuru, S. C. K.; Wagenaar, M.; O'Donnell, C. J.; Lam, M.-H.; Musto, S.; Loganzo, F. New Cytotoxic Benzosuberene Analogs. Synthesis, Molecular Modeling and Biological Evaluation. *Bioorg. Med. Chem. Lett.* **2013**, *23*, 6688–6694.

(26) Pinney, K. G.; Sriram, M.; George, C.; Tanpure, R. P. Efficient Method for Preparing Functionalized Benzosuberenes. US20120130129 A1, May 24, 2012.

(27) Tanpure, R. P.; George, C. S.; Sriram, M.; Strecker, T. E.; Tidmore, J. K.; Hamel, E.; Charlton-Sevcik, A. K.; Chaplin, D. J.; Trawick, M. L.; Pinney, K. G. An Amino-Benzosuberene Analogue That Inhibits Tubulin Assembly and Demonstrates Remarkable Cytotoxicity. *MedChemComm* **2012**, *3*, 720–724.

(28) Rischin, D.; Bibby, D. C.; Chong, G.; Kremmidiotis, G.; Leske, A. F.; Matthews, C. A.; Wong, S. S.; Rosen, M. A.; Desai, J. Clinical, Pharmacodynamic, and Pharmacokinetic Evaluation of BNC105P: A Phase I Trial of a Novel Vascular Disrupting Agent and Inhibitor of Cancer Cell Proliferation. *Clin. Cancer Res.* **2011**, *17*, 5152–5160.

(29) Flynn, B. L.; Gill, G. S.; Grobelny, D. W.; Chaplin, J. H.; Paul, D.; Leske, A. F.; Lavranos, T. C.; Chalmers, D. K.; Charman, S. A.; Kostewicz, E.; Shackleford, D. M.; Morizzi, J.; Hamel, E.; Jung, M. K.; Kremmidiotis, G. Discovery of 7-Hydroxy-6-Methoxy-2-Methyl-3-(3,4,5-Trimethoxybenzoyl)benzo[*b*]furan (BNC105), a Tubulin Polymerization Inhibitor with Potent Antiproliferative and Tumor Vascular Disrupting Properties. *J. Med. Chem.* **2011**, *54*, 6014–6027.

(30) Nowak, A. K.; Brown, C.; Millward, M. J.; Creaney, J.; Byrne, M. J.; Hughes, B.; Kremmidiotis, G.; Bibby, D. C.; Leske, A. F.; Mitchell, P. L. R.; Pavlakis, N.; Boyer, M.; Stockler, M. R. A Phase II Clinical Trial of the Vascular Disrupting Agent BNC105P as Second Line Chemotherapy for Advanced Malignant Pleural Mesothelioma. *Lung Cancer* **2013**, *81*, 422–427.

(31) Flynn, B. L.; Verdier-Pinard, P.; Hamel, E. A Novel Palladium-Mediated Coupling Approach to 2,3-Disubstituted Benzo[b]thiophenes and Its Application to the Synthesis of Tubulin Binding Agents. *Org. Lett.* **2001**, *3*, 651–654.

(32) Flynn, B. L.; Hamel, E.; Jung, M. K. One-Pot Synthesis of Benzo[b]furan and Indole Inhibitors of Tubulin Polymerization. *J. Med. Chem.* **2002**, *45*, 2670–2673.

(33) Kremmidiotis, G.; Leske, A. F.; Lavranos, T. C.; Beaumont, D.; Gasic, J.; Hall, A.; O'Callaghan, M.; Matthews, C. A.; Flynn, B. BNC105: A Novel Tubulin Polymerization Inhibitor That Selectively Disrupts Tumor Vasculature and Displays Single-Agent Antitumor Efficacy. *Mol. Cancer Ther.* **2010**, *9*, 1562–1573.

(34) Garon, E. B.; Kabbinavar, F. F.; Neidhart, J. A.; Neidhart, J. D.; Gabrail, N. Y.; Oliveira, M. R.; Lu, S. P.; Balkissoon, J. Randomized Phase II Trial of a Tumor Vascular Disrupting Agent Fosbretabulin Tromethamine (CA4P) with Carboplatin (C), Paclitaxel (P), and Bevacizumab (B) in Stage IIIb/IV Nonsquamous Non-Small Cell Lung Cancer (NSCLC): The FALCON Trial. *J. Clin. Oncol.* **2010**, *28:15s*.

(35) Sosa, J. A.; Elisei, R.; Jarzab, B.; Bal, C. S.; Koussis, H.; Gramza, A. W.; Ben-Yosef, R.; Gitlitz, B. J.; Haugen, B.; Karandikar, S. M.; Khuri, F. R.; Licitra, L. F.; Remick, S. C.; Marur, S.; Lu, C.; Ondrey, F. G.; Lu, S.; Balkissoon, J. A Randomized Phase II/III Trial of a Tumor Vascular Disrupting Agent Fosbretabulin Tromethamine (CA4P) with Carboplatin (C) and Paclitaxel (P) in Anaplastic Thyroid Cancer (ATC): Final Survival Analysis for the FACT Trial. *J. Clin. Oncol.* **2011**, *29: 2011 (suppl; abstr 5502)*.

(36) Leighl, N. Classification and Toxicities of Vascular Disrupting Agents. *Clin. Lung Cancer* **2011**, *12*, 18–25.

(37) Wu, X.-Y.; Ma, W.; Gurung, K.; Guo, C.-H. Mechanisms of Tumor Resistance to Small-Molecule Vascular Disrupting Agents: Treatment and Rationale of Combination Therapy. *J. Formos. Med. Assoc.* **2013**, *112*, 115–124.

(38) Huang, B.; Desai, A.; Tang, S.; Thomas, T. P.; Baker, J. R. The Synthesis of a c(RGDyK) Targeted SN38 Prodrug with an Indolequinone Structure for Bioreductive Drug Release. *Org. Lett.* **2010**, *12*, 1384–1387.

(39) De Groot, F. M. H.; de Bart, A. C. W.; Verheijen, J. H.; Scheeren, H. W. Synthesis and Biological Evaluation of Novel Prodrugs of Anthracyclines for Selective Activation by the Tumor-Associated Protease Plasmin. *J. Med. Chem.* **1999**, *42*, 5277–5283.

(40) Dubowchik, G. M.; Mosure, K.; Knipe, J. O.; Firestone, R. A. Cathepsin B-Sensitive Dipeptide Prodrugs. 2. Models of Anticancer Drugs Paclitaxel (Taxol®), Mitomycin C and Doxorubicin. *Bioorg. Med. Chem. Lett.* **1998**, *8*, 3347–3352.

(41) Jeffrey, S. C.; De Brabander, J.; Miyamoto, J.; Senter, P. D. Expanded Utility of the B-Glucuronide Linker: ADCs That Deliver Phenolic Cytotoxic Agents. *ACS Med. Chem. Lett.* **2010**, *1*, 277–280.

(42) Shen, B.-Q.; Xu, K.; Liu, L.; Raab, H.; Bhakta, S.; Kenrick, M.; Parsons-Reponte, K. L.; Tien, J.; Yu, S.-F.; Mai, E.; Li, D.; Tibbitts, J.; Baudys, J.; Saad, O. M.; Scales, S. J.; McDonald, P. J.; Hass, P. E.; Eigenbrot, C.; Nguyen, T.; Solis, W. A.; Fuji, R. N.; Flagella, K. M.; Patel, D.; Spencer, S. D.; Khawli, L. A.; Ebens, A.; Wong, W. L.; Vandlen, R.; Kaur, S.; Sliwkowski, M. X.; Scheller, R. H.; Polakis, P.; Junutula, J. R. Conjugation Site Modulates the in Vivo Stability and Therapeutic Activity of Antibody-Drug Conjugates. *Nat. Biotechnol.* **2012**, *30*, 184–189.

(43) De Groot, F. M. H.; van Berkom, L. W. A.; Scheeren, H. W. Synthesis and Biological Evaluation of 2‘-Carbamate-Linked and 2‘-Carbonate-Linked Prodrugs of Paclitaxel: Selective Activation by the Tumor-Associated Protease Plasmin. *J. Med. Chem.* **2000**, *43*, 3093–3102.

(44) De Groot, F. M.; Loos, W. J.; Koekkoek, R.; van Berkom, L. W.; Busscher, G. F.; Seelen, A. E.; Albrecht, C.; de Bruijn, P.; Scheeren, H. W. Elongated Multiple Electronic Cascade and Cyclization Spacer Systems in Activatible Anticancer Prodrugs for Enhanced Drug Release. *J. Org. Chem.* **2001**, *66*, 8815–8830.

(45) Dubowchik, G. M.; Firestone, R. A.; Padilla, L.; Willner, D.; Hofstead, S. J.; Mosure, K.; Knipe, J. O.; Lasch, S. J.; Trail, P. A. Cathepsin B-Labile Dipeptide Linkers for Lysosomal Release of Doxorubicin from Internalizing Immunoconjugates: Model Studies of Enzymatic Drug Release and Antigen-Specific In Vitro Anticancer Activity. *Bioconjug. Chem.* **2002**, *13*, 855–869.

(46) Shaikh, A.-A. G.; Sivaram, S. Organic Carbonates. *Chem. Rev.* **1996**, *96*, 951–976.